Novel sex-biased outcomes in neuroblastoma are associated with distinct gene expression and chromosomal loss patterns.

Vishwa Patel[1*], Mariya Raleigh[1*], Lorraine-Rana E. Benhamou[2], Xin Shen[1], Erika C. Espinosa[2], Niharika R. Badi[2], Dennis A. Sheeter[2], and John T. Powers[1,2]

[1]Division of Pharmacology and Toxicology, College of Pharmacy, The University of Texas at Austin, 78712
[2]Dell Pediatric Research Institute, Department of Pediatrics, Dell Medical School at The University of Texas at Austin, 78723
*VP and MR contributed equally to this work
Correspondence: J. T. Powers, john.powers@austin.utexas.edu, ORCID 0000-0003-1598-2417

Email/ORCID:
V. Patel, vishwa.patel@utexas.edu, ORCID 0000-0003-0418-134X
M. Raleigh, mariya.raleigh@austin.utexas.edu, ORCID 0009-0006-0975-2286
L-R.E. Benhamou, lorrainerana.benhamou@austin.utexas.edu, ORCID 0009-0002-6443-9269
X. Shen, calandrashen@utexas.edu, ORCID 0000-0002-4195-560X
E.C. Espinosa, ece97@austin.utexas.edu
N.R. Badi, niharikareddy.badi@austin.utexas.edu
D.A. Sheeter, dennis.sheeter@austin.utexas.edu, ORCID 0009-0006-0412-0546

Abstract

The worst patient outcomes in neuroblastoma are driven by high-risk disease[1,2], which is divided into similarly sized *MYCN* amplified and *MYCN* non-amplified patient subgroups[3]. Male patients have been reported to have slightly worse outcomes than females in all-patient analyses of large patient studies[3,4]. However, we show here that in *MYCN* non-amplified high-risk and stage 4s low-risk disease, female patients have significantly worse overall survival than males. Female *MYCN* non-amplified high-risk patients highly express *H19* and *DLK1*, both of which drive cell growth *in vitro* and associate with worse outcomes in females, but not males. Further, chromosome-specific expression analysis of these patients reveals broad sex disparities in chromosomal patterning, including female-specific retention of chromosome 11q, a pattern typically reserved for *MYCN*-amplified disease[5,6]. Finally, we show that *H19*, a known *let-7* microRNA target[7], sequesters *let-7* in females, providing a rationale for worse female survival and reconciling retention of chromosome 11q. We propose that this novel sex-based outcome disparity is driven by *let-7* inhibition, confirming and expanding on a model of neuroblastoma development where *let-7* mitigation is central to disease pathology[8].

Introduction

Neuroblastoma (NB) is the most common extracranial solid tumor in children that arises from the neural crest lineage[9,10]. Survival rates in NB are highly dependent upon tumor risk group classification. According to the Children's Oncology Group risk system, NB tumors can be subdivided into low-risk (LR), intermediate-risk (IR), or high-risk (HR) groups based on stage, patient age, favorability of histology, *MYCN* status, and presence of other genetic aberrations such as ploidy or chromosomal loss[11,12]. LR and IR NB have favorable overall survival (90-95%), as do stage 4s tumors which often regress without intervention[10,13,14]. Unfortunately, HR disease is notoriously difficult to treat and has an OS rate below 50%[15,16]. Consequently, HR NB patients endure one of the most intensive genotoxic therapeutic regimens in all of oncology[17], and those that do survive are often left with life-long complications and increased risk for secondary cancers. Thus, an increased understanding of the genetic drivers of HR disease will aid in better classification and stratification of patients and in the development of more effective, less genotoxic treatments for high-risk neuroblastoma patients. Possibly leading to increased patient survival and improved quality of life for survivors.

While some sex and racial disparities have been described in overall patient outcomes[3,4,18–21], it has been difficult to determine what drives these differences due to the level of interrogation and available annotations within patient datasets. Studies that assess potential sex and racial biases oftentimes only account for overall outcomes. This broad-stroke method of analyzing patient datasets hinders researchers' understanding of cancers with complex genetic

subgroupings such as NB. More comprehensive patient annotation will enable the identification of more refined subcategories of NB outcomes and associated genetics. This will facilitate a deeper understanding of the genetic programs that drive subpopulations, leading to improved discovery of novel therapeutic targets. Large-scale NB patient outcomes studies often report that male patients' outcomes are slightly but significantly worse than for females. While the absolute numbers associated with these conclusions are correct, it is also true that the incidence of NB itself and HR disease is higher in males. On a per-patient basis, male and female outcomes have not been directly investigated, in particular within important patient groups like HR patients or within the *M-Amp* and *M-Non* HR sub-groups.

In addition to the overarching risk categorization of NB, further patient stratification occurs based on distinct genetic patterning within risk groups. For example, HR disease is further subdivided by the presence or absence of *M-Amp. MYCN* is part of a small oncogene family that includes *c-MYC* and *l-MYC* and is the main oncogene of NB. *MYCN* overexpression, outside of embryonal development, drives increased cellular proliferation and contributes to tumorigenesis[17]. *MYCN* status is correlated with the presence of other common and central genetic and chromosomal alterations in NB, such as deletions of 1p and 11q, 14q loss, 17q gain, and triploidy. *MYCN* mRNA is targeted by the *let-7* tumor suppressor microRNA family, which consists of nine *let-7* family members spread across multiple genetic loci[22]. We previously showed that high levels of *MYCN* mRNA in *MYCN*-amplified disease turn the tables on *let-7*, where the 3′ UTR of *MYCN* mRNA efficiently sequesters *let-7*, thus inhibiting its function[8,23]. This discovery further provided an explanation for the longstanding observation that Chr 11q, known to harbor the most highly expressed *let-7* locus (*let-7a-2*), is frequently lost in *M-Non*, but not in *M-Amp* disease. This work established that higher levels of Chr 11q-derived *let-7a* are functionally impaired by *MYCN* mRNA. This discovery demonstrated for the first time that, through microRNA sequestration, an oncogenic mRNA can independently contribute to both oncogenicity and selective genetic patterning in cancer.

Here, we set out to assess potential sex- and race biases in NB. We discovered a striking sex bias in patient outcomes in *M-Non*/HR disease that is associated with *H19* and *DLK1* deregulation. Biased outcomes were also identified in *M-Non* stage 4s disease, as well as a surprising opposing sex bias negatively affecting male African American patients. We also identified significant differences in chromosomal loss patterns between *M-Non*/HR female and male patients using a novel analytic approach to differential gene expression. Finally, we connect this novel sex-biased OS outcomes with chromosomal loss patterns and *let-7* sequestration by *H19*, expanding on our previous report on the intersection between *MYCN* expression, *let-7* inhibition, and chromosomal patterning in *M-Amp* disease[8,23].

Results

Female neuroblastoma patients have worse overall survival in High-Risk MYCN Non-Amplified disease.

Overall, NB incidence and the occurrence of HR disease are slightly higher in males than in females[3,4,24]. Despite this disparity of frequency, an in-depth analysis of female *vs.* male outcomes in HR disease has yet to be reported. We therefore first assessed potential sex bias in multiple NB clinical subsets through analysis of a 498-patient cohort (SEQC) with sufficient annotation to simultaneously interrogate risk stratification, *MYCN* status, and patient sex[25]. No difference in OS between the sexes was observed in this and two additional datasets (TARGET, Kocak) when risk status was not considered (***Supplementary Table 1, Extended Data Fig. 1a, 1b, 1c***)[26,27]. The 64% of SEQC patients with LR disease also exhibited no significant difference in survival between males and females (***Figure 1a***, top right panel). However, among the remaining HR patients, females displayed a striking pattern of significantly worse OS ($p = 0.0075$, ***Figure 1a***, top left). Analysis of the *M-Amp* and *M-Non* HR subgroups revealed significantly worse OS in female *M-Non*/HR patients ($p = 0.021$), as opposed to similar outcomes for females and males in the *M-Amp*/HR subgroup (***Figure 1a***, lower right and left panels, respectively).

We next sought to validate this finding in additional datasets. The Kocak NB patient study has annotations for *MYCN* status, patient age, stage, and sex but is not annotated for risk status (***Supplementary Table 1***). To approximate HR disease[4], we compared female and male OS in stage 3 or stage 4 patients older than 18 months and again observed that higher-risk, late-stage female NB patients had significantly worse OS ($p = 0.0037$, **Extended *Data Fig. 2a***). We then assessed female and male OS in the TARGET NB study, which is exceptionally well-annotated (***Supplementary Table 1***). An initial comparison of HR patients yielded no difference in outcomes between female and male patients, which extended to both the *M-Amp* and *M-Non* HR subgroups (***Extended Data Fig. 2b***). The TARGET study is so well annotated

as to include reports of patient race. Given that the Germany-based Kocak study has a strong Caucasian patient bias (*personal communication*), we reasoned that race may contribute to our failed validation. Over 12% of the TARGET study patients are African American (AA), representing the second largest race group in the study. Upon exclusion of these patients from our analysis, we once again observed the same pattern of significantly worse OS in female *M-Non*/HR patients as we saw in the SEQC study (***Extended Data Fig. 2c***). However, when we then analyzed the AA patient group (n = 31), we observed a striking, yet opposite sex-bias in OS, where male HR patients have dramatically worse OS (93% DFD) than females (***Figure 1b***).

Analysis of *M-Non* stage 4s patients, whose prognosis is overall favorable, also revealed a significant difference in OS outcomes in females and males. When analyzed individually, females in the SEQC and Kocak cohorts had significantly worse OS than male *M-Non* stage 4s patients ($p = 0.019, 0.021$, respectively, ***Extended Data Fig. 3a, 3b***). A third study revealed a similar trend but did not achieve significance ($p = 0.17$, **Extended *Data Fig. 3c***). When patient data from these three studies was combined into a single Kaplan-Meier analysis, a strong sex bias emerged where females performed much worse than male 4s patients ($p = 0.00076$, **Figure *1c***). In fact, the only patients who died within this group were female (8/49 patients), while there were no male deaths at all (0/85 patients) (***Figure 1c***). This is surprising given that stage 4s disease has an excellent prognosis, with over 90% survival and close to 50% spontaneous regression[28]. Our results suggest a near 100% survival rate in *M-Non* stage 4s male patients, compared to 16.4% death in females (***Figure 1c***).

To complete our analysis with better numbers of female *vs.* male *M-Non* HR patients, we next combined all relevant HR patients from the SEQC, Kocak, and TARGET (AA patients excluded) studies and observed a statistically improved confirmation of our female-biased OS in HR disease (n = 461 patients, $p = 1.3 \times 10^{-5}$, ***Figure 1d***). Furthering this analysis on *M-Non*/HR patients once again yielded a stronger representation of sex-biased OS in female *M-Non*/HR disease (n = 271, $p = 4.3 \times 10^{-4}$, ***Figure 1e***).

H19 and DLK1 are associated with poor survival in female, but not male, neuroblastoma patients.

Next, we analyzed gene expression patterns in *M-Non*/HR/DFD female (n = 14) and male (n = 26) patients from the SEQC study. As expected, the top five hundred genes in female patients from this group are strongly shifted in an X-Y plot of differential gene expression towards female enriched expression (***Figure 2a***, right panel). In contrast, this gene set lined up midline between female and male patients in *M-Amp*/HR and *M-Non*/LR living patients, showing a lack of enrichment of these genes in females from those clinical subgroups (***Figure 2a***, middle and left panels, respectively). This suggests that female *M-Non*/HR/DFD patients may have a distinct gene expression signature. Among the top twenty genes upregulated in these females, the long noncoding RNA *H19* and delta-like non-canonical Notch ligand 1 (*DLK1*) emerged as the most upregulated non-Chr X genes (***Figure 2a***, right panel, ***Extended Data Fig. 4a*** left panels, ***Supplemental Table XXX***). Further, *H19* and *DLK1* expression is significantly correlated in females (r = 0.52, p = 0.019) but not male *M-Non*/HR patients, suggesting a degree of co-expression in female patients (***Figure 2c***). A similar analysis of HR-approximated patients in the Kocak study again showed that *H19* and *DLK1* are significantly upregulated in female patients (***Figure 2b, Extended Data Fig. 4a*** right panels, ***Supplemental Table YYYY?***). Further, despite very small patient numbers (n = 5 female, 6 male), a comparison of *H19* and *DLK1* expression in *M-Non* stage 4s patients with progressive disease shows higher, although not significantly so, expression in female patients (***Extended Data Fig. 4b***). Of note, expression of *H19* and *DLK1* in the adrenal medulla is among the highest for all tissues (***Extended Data Fig. 5***), introducing the possibility that high *H19* and *DLK1* expression in female *M-Non*/HR patients may represent sex-specific, retained expression from a common NB tissue of origin. Cox-regression analysis of OS Hazard Ratios of the top twenty female-enriched non-X Chr genes reveals that *DLK1*, *H19* (and its embedded microRNA, *miR-675*), are significantly associated with worse outcomes in female but not male patients (***Figure 2d***). This association was validated through Kaplan-Meier analysis of *M-Non* patients in the SEQC and Kocak studies (***Extended Data Fig. 6a, 6b***). No association with female or male outcomes was noted in *M-Amp* disease in patients from either the SEQC or Kocak studies (***Extended Data Fig. 7***).

Both *H19* and *DLK1* have been reported as oncogenes in multiple cancers[29–32]. To assess their ability to promote tumor growth in NB, we over-expressed both in murine 3T3 and human SH-SY5Y cells. Expressing *H19* as either an intact, mature lncRNA sequence (*H19*), or as a full-length genetic locus version containing endogenous introns (*H19-GL*) in

both cell types resulted in higher growth rates compared to GFP control cells (***Figure 2e***). Similar results were observed with *DLK1* overexpression in 3T3 and SHSY-5Y (***Figure 2e***). We next used small interfering RNAs (siRNAs) individually or in tandem in *M-Non* SH-SY5Y cells and noted significant and additive growth inhibition with *H19* and *DLK1* knockdown (***Extended Data Fig. 8***). To confirm this observation, we used a CRISPR/Cas9-mediated gene disruption growth assay modeled on classical large-scale dropout screens to disrupt *H19* and *DLK1* genetically. Cas9 expressing SH-SY5Y and SK-N-F1 *M-Non* NB cells were transfected with single guide RNA (gRNA) constructs co-expressing either GFP and a single non-targeting gRNA or mCherry and single gRNAs targeting *RPL3*, *DLK1*, or *H19*. A third *H19*-targeting gRNA directly targets *miR-675* located within the first exon. Cells transfected with gRNAs on day zero were then assayed for fluorescence-positive cells by flow cytometry over time to assess the potential loss of fluorescent cells. Neither cell line displayed significantly altered GFP fluorescence, as compared to a profound reduction driven by both positive control *RPL3* gRNAs (***Figure 2g***). Similarly, *DLK1* and *H19* targeting gRNAs resulted in significant fluorescence reduction, validating our siRNA results. These data suggest that *H19* and *DLK1* drive more aggressive tumor cell growth, thereby contributing to the poor outcomes we report in *M-Non*/HR female patients.

Differential gene expression analysis reveals striking sex-biased chromosomal loss patterns.

When we noted the genomic location of the top 500 genes significantly increased in female *M-Non*/HR/DFD patients, we noticed a strong enrichment for genes residing in the q arm of Chr 11 (15.8%). We then assessed enrichment by chromosomal location for those that represented more than 10% of the top 500 genes. Female-biased gene expression was also noted for Chr 4 (10.8%) and Chr 12q (10.2%) (***Figure 3a,*** *bottom panel*). This prompted us to examine the chromosomal distribution of male-enriched genes, where we observed an overrepresentation of Chr 1p (10.6%) and Chr 19 (11.4%). (***Figure 3a,*** *top panel*). We reasoned that these enrichment patterns may suggest actual chromosomal patterning differences between female and male *M-Non*/HR/DFD patients. In order to examine this directly, we first assessed differential expression patterns in M-Amp vs. M-Non NB patients, where chromosomal patterns are well established. First, looking at Chr 13, not known to have a differential Chr loss signature in *M-Amp* vs. *M-Non* NB, we observed an expected lack of significant difference in gene expression by volcano plot and paired t-test (***Figure 3b***). However, when we looked at Chr 1p (bp 1-80e6), which is known to be lost in almost all *M-Amp* disease [6,33], we saw a dramatic shift of gene expression toward the *M-Non* group, which is consistent with the known Chr 1p loss pattern ($p = 8.4 \times 10^{-100}$, ***Figure 3c***). Next, when we looked at Chr 11q (bp 80e6-q/ter), which is known to be frequently lost in *M-Non* disease[5,6,8,34], we observed a significant shift in gene expression towards *M-Amp* disease, again consistent with known chromosomal patterning ($p = 0.0028$, ***Figure 3d***). This analysis establishes that we can faithfully recapitulate known relative chromosomal patterns between patient groups, thus allowing us to use this method to identify novel chromosomal abnormalities.

Using Chr 13 as a negative control, as Chr 13 genes were not enriched in either female or male patients (1% and 0.6%, respectively (***Figure 3a***, ***Supplemental Data Table XXX***), we observed no significant sex bias in gene expression in *M-Non*/HR/DFD patients from the SEQC study or in stage 4/ older than 18 months patients from the Kocak study (***Figure 3e***). Next, we examined Chr 1p (bp 1-80e6) and observed a significant shift toward male patients in both the SEQC and Kocak patient groups ($p = 1.8 \times 10^{-34}$, 2.3×10^{-5}, *respectively,* ***Figure 3f***). Further, analysis of Chr 11q genes (bp 80e6-q/ter) showed a significant shift in gene expression towards female patients in both studies ($p = 2.9 \times 10^{-33}$, 1.1×10^{-17}, *respectively,* ***Figure 3g***). Other chromosomal enrichment patterns identified across Chr 4, Chr 12q, and Chr 19 (***Figure 3a***) also showed significant sex-biased volcano plot shifts (***Extended Data Figure 9***). These results demonstrate for the first time that sex-biased patterns of chromosomal loss exist in NB. While this analysis does not allow for de novo determination of directionality for a given chromosomal imbalance, Chr 1p and 11q are very well-known within NB, and it is highly likely that the patterns we observed are indeed due to loss within the deficient group[5,6,34–37]. In addition, Chr 4[35,36,38] and Chr 12q[39–41] loss have been reported to be associated with poor outcomes in NB, which is consistent with the female-biased poor OS we observed in M-Non/HR disease. Whole Chr 19 gain[35] has been reported to be associated with better outcomes, suggesting that we may have identified a pattern of Chr 19 gain in males as opposed to Chr 19 loss in females. These observations show that we can faithfully re-derive known differential chromosomal patterns between patient groups and identify novel chromosomal imbalances as well.

Finally, we examined the local genomic regions near both *DLK1* and *H19* and observed that the Chr 14q region near the *DLK1* locus is associated with a female-enriched shift, suggesting a genetic dose difference in favor of females for that region (***Extended Data Figure 10a***). *H19*, on the other hand, showed no significant shift in either direction (***Extended Data Figure 10b***). This discrepancy suggests that *DLK1* elevation in females may be due, at least in part, to differences in gene copy number, whereas elevated *H19* expression may be through a more direct mechanism in females.

H19 inhibits let-7 in female M-Non/HR patients in a manner similar to MYCN mRNA in M-Amp disease.

Despite their *MYCN* status, female *M-Non*/HR/DFD patients appear to have a similar Chr 1p/Chr 11q chromosomal pattern to that of *M-Amp* patients. To explore this further, we repeated our differential chromosome-specific gene expression analysis of Chr 13, Chr 1p, and Chr 11q in male and female NB patients. *M-Amp* male patients displayed the expected pattern, revealing loss of Chr 1p and retention of Chr 11q compared to the *M-Non* group (***Figure 4a***, upper panels). Female patients showed similar patterns for Chr 13 and Chr 1p but diverged for Chr 11q, showing a mildly significant shift towards *M-Non* patients. This suggests that female *M-Non* patients may indeed retain Chr 11q more than male patients, as we demonstrated in ***Figures 3f*** and ***3g***, and further supports the novel idea that *M-Non*/HR females may display a classically *M-Amp* loss pattern for Chr 1p and Chr 11q.

We previously established that in *M-Amp* NB, *MYCN* mRNA, which is a *let-7* microRNA target (***Figure 4b***), sequesters *let-7* in *M-Amp* disease. Thereby mitigating its function and relieving the selective pressure to lose Chr 11q, which houses one of the highest expressed *let-7* loci, *let-7a-2*[8] (***Figure 4b, Extended Data Figure 11a, 11b***). This work provided a mechanism by which Chr 11q is retained in *M-Amp* NB but preferentially lost in *M-Non* disease, establishing that noncoding elements within a protein-coding mRNA can have autonomous oncogenic function with genetic consequences. Our observation that female *M-Non*/HR patients have a Chr 11q pattern that matches classical *M-Amp* patterning may have consistencies with this original discovery. *H19*, which is highly expressed in these female patients (***Figure 2a, Extended Data Figure 4***), is known to contain four *let-7* sites (***Figure 4d***)[7] and has been reported to sequester *let-7*[42–45]. *H19* shares several characteristics in NB with *MYCN*, a known *let-7* sponge. As expected, *MYCN* correlates with *let-7* levels across *M-Amp* and *M-Non* NB cell lines (***Figure 4c***, *left panel*)[8]. Similarly, *H19* correlates with *let-7* levels in *M-Non* NB cell lines (***Figure 4c***, *right panel*). This relationship holds with regard to the *let-7a-2* host gene, *MIR100HG*, in human NB patients, where *MYCN* levels correlate with *MIR100HG* in HR NB patients (***Figure 4b*** and ***4d***, *left panel*). *H19* levels also positively correlate with *MIR100HG* expression in *M-Non* HR disease, but only in females (***Figure 4d***, *right panel*). This suggests that *H19* may play a role in *let-7* inhibition in only female *M-Non*/HR patients, which unites the sex-based disparity in OS with the Chr 11q (*let-7a-2*) patterning we observed.

To test this more directly, we examined the expression levels of a representative set of *let-7* targets in *H19* and *H19-GL* expressing SHSY-5Y cells. Compared to GFP, *H19*-expressing cells all showed significantly higher expression of every *let-7* target tested (***Figure 4e***). *H19-GL* expressing cells displayed a similar pattern, with all but three primer sets (*LIN28B*, *ZBTB10*, and *SKIL*) registering significantly higher *let-7* target expression (***Figure 4e***). In general, *H19-GL* resulted in lower levels of *let-7* target enrichment, which is consistent with lower levels of mature *H19* in *H19-GL* vs. *H19* expressing SHSY-5Y cells (***Extended Data Figure 11c***). Consistent with these in vitro results, female *M-Non*/HR/DFD NB patients have significantly enriched expression of *let-7* target mRNAs containing two or more *let-7* sites (*n = 133 let-7 targets*, ***Extended Data Figure 11d***). Next, we examined the effect of H19 depletion on *let-7* target mRNA. Using two different siRNAs, we knocked down *H19* in SK-N-F1 *M-Non* NB cells (***Extended Data Figure 12a***) and observed significantly decreased expression of all nine *let-7* target mRNAs (***Extended Data Figure 12b***). These results suggest that *H19* serves to sequester and inhibit *let-7* in female *M-Non*/HR/DFD patients, similar to how *MYCN* sequesters relatively high *let-7* levels in *M-Amp* disease[8]. They similarly provide a plausible rationale for worse female outcomes, again mirroring the impact of *M-Amp*-specific *MYCN* mRNA-mediated *let-7* inhibition. This novel role for *H19* in female NB patients provides a selective mechanism by which these female patients tend to retain Chr 11q, a pattern previously only associated with *M-Amp* patients.

Discussion

Understanding the origins and driving mechanisms behind the sex-based disparity in OS described here may lead to an improved understanding of female-specific cancer genetics and sex-specific approaches to therapy, a first for NB.

Using a targeted analysis of genetic, sex, and race annotations allowed us to discover a novel and striking female-biased outcome pattern in *M-Non*/HR patients. While primarily male-biased, worse outcomes have been reported in over twenty cancer types[46,47], the majority of these disparities were identified by looking at all patients within a given cancer[47]. Given the results of our own compartmentalized analysis, we predict that sex biases are more widespread in human cancers, that these biases will be more divergent in some patient subgroups, and that the directionality may change depending on the subgroup in question. The results of our analysis provide a rationale for widespread sub-group analysis across most if not all, tumor types. Important differences within patient subsets can be hidden within all-patient OS analyses. It is therefore imperative to consider tractable patient subgroups when performing patient outcomes analysis. In addition, to facilitate such subgroup-focused analysis, we must strive to maximize annotation when performing large-scale patient studies. Of eight patient datasets available for possible outcomes analysis on the r2 database, only four listed patient sex within their available annotations[48]. In contrast, the TARGET study with only 249 patients was annotated to the degree that it included patient race, allowing us to discover an additional and opposite-sex bias in African American patients (***Figure 4***).

Both *H19* and *DLK1* have been implicated as oncogenes in multiple cancers[29–32,49–53]. *H19* is a long non-coding RNA with multiple functions, including regulation of gene expression and microRNA sequestration[49,54]. *DLK1*, a transmembrane protein involved in the highly conserved NOTCH signaling pathway, can function as a non-canonical NOTCH ligand to exert control over cell-to-cell communication, proliferation, and differentiation[29,30]. We found similar and robust pro-growth functions for both *H19* and *DLK1* in murine 3T3 embryonic fibroblasts and in human *M-Non* SHSY-5Y, SK-N-F1, and CHLA-42 NB cells (***Figure 2e***, ***2f***, ***2g***, and ***Extended Data Figure 8***). The local organization of the *H19* (*h*) and *DLK1* (*d*) loci are remarkably similar. They both reside in areas of imprinted genes and are part of a ~200kb local segment comprised of a protein-coding gene (*DLK1*(*d*) or *IGF2*(*h*), both imprinted), followed by long noncoding RNA (*MEG3*(*d*) or *H19*(*h*), both imprinted), followed by another protein-coding gene (*RTL1*(*d)* or *MRPL23*(*h*))[55,56]. These similarities suggest the possibility of shared regulation.

NB is a disease of genetic compartmentalization, both in terms of expression patterns of key genes and repeating patterns of chromosomal gains and losses. We identified a surprising sex disparity in chromosomal imbalance across multiple chromosomes, including Chr 1p and Chr 11q (Figure ***3a***, ***3f***, and ***3g***). This observation revealed an unexpected alignment between female *M-Non*/HR and classical *M-Amp* patterning, as both groups appear to lose Chr 1p and retain Chr 11q. This pattern was validated upon sex-directed analysis of *M-Amp* vs. *M-Non* NB patients (***Figure 4a***). Our previous work established that in *M-Amp* NB, *MYCN* mRNA, which contains two *let-7* sites, efficiently sequesters *let-7* and inhibits its function[8,23]. This work provided the first plausible explanation that Chr 11q, which harbors the most highly expressed *let-7* locus (*let-7a-2*), is frequently lost in *M-Non*, but not in *M-Amp* disease. This work showed for the first time that noncoding elements with an oncogenic mRNA can independently contribute to both tumor pathology and selective genetic patterning in cancer[8]. The alignment between female *M-Non*/HR and *M-Amp* patterns led us to discover that *H19*, known to have four *let-7* sites[7], sequesters *let-7* in female *M-Non*/HR patients in a manner mirroring that of *MYCN* in *M-Amp* disease. This observation provides a rationale for the observed female retention of Chr 11q in *M-Non*/HR disease. The mechanistic similarity of noncoding *H19* and *MYCN* mRNA function validates our earlier work and suggests that sequestration of *let-7* by either 3'UTRs of protein-coding mRNAs or *let-7* sites within long noncoding RNAs may be a fundamental mechanism of *let-7* mitigation in NB and other cancers.

We show here significant sex- and race-based disparities in OS relative to *MYCN* status in NB through analysis of multiple publicly available patient datasets with good to excellent patient annotations. This discovery provides a novel way to consider how incidence and genetic patterning intersect with disease pathology and patient outcomes in a genetically and clinically heterogeneous disease like NB. Our findings demonstrate the value of highly compartmentalized cohort analysis of large, well-annotated patient datasets. Further, given the frequency and consistency of multiple genetic events in NB, these findings establish a novel paradigm of sex-biased outcomes and chromosomal patterning in NB and solidify the centrality of *let-7* mitigation, which has broad implications for human malignancy.

Methods

R2 database: Human NB patient RNA-seq, microarray, and overall survival data sets were obtained from the r2: microarray analysis and visualization platform (http:// r2.amc.nl)[48]. Data sets were used for analysis: SEQC498 (GEO accession number GSE62564)[25], Kocak649 (GEO accession number GSE45547)[26], Cavalli673 (GEO accession number GSE85217)[57], TARGET249 (r2 internal identifier: ps_avgpres_targetnrbl249_huex10t); results from analysis of the TARGET249 dataset are based upon data generated by the Therapeutically Applicable Research to Generate Effective Treatments (https://www.cancer.gov/ccg/research/genome-sequencing/target) initiative (phs000467)[27].

Cell Culture: The neuroblastoma cell lines, including CHLA-15 (RRID CVCL_6594), CHLA-20 (RRID CVCL_6602), KAN (SMS-KAN, RRID CVCL_7131), KANR (SMS-KANR, RRID CVCL_7132), KCN (SMS-KCN, RRID CVCL_7133), KCNR (SMS-KCNR, RRID CVCL_7134), and SK-N-F1 (RRID CVCL-1702), were obtained from the Childhood Cancer Repository at the Texas Tech University Health Science Center, a partner of the Children's Oncology Group. All cells were cultured in media as recommended by COG. Additionally, BJ fibroblasts (NHF, ATCC CRL-2522), SH-SY-5Y (ATCC CRL-2266), and BALB/3T3 (ATCC CCL-163.2) were cultured in RPMI-1640 media supplemented with 10% heat-inactivated fetal bovine serum (HI-FBS). Cells were grown at 37°C and 5% CO_2. All cell lines were acquired or purchased for this study and are not among the commonly misidentified ones. They were routinely tested and found negative for mycoplasma contamination.

Plasmids: Control *GFP* vector (pPB[Exp]-Puro-EF1A>EGFP); *H19* pPB[ncRNA]-EGFP-EF1A>hH19[NR_002196.2]; *H19-GL*: pBP[ncRNA]-EGFP-EF1a>{h19 full length NR_002196.2}; and *DLK1* (pPB[Exp]-mCherry-SFFV>hDLK1[NM_003836.7]) vectors were designed and purchased from vectorbuilder.com. 3T3 and SHSY-5Y cells were co-transfected with 1ug of an above plasmid and a hyPBase transposase-expressing vector (pRP[Exp]-mCherry-CAG>hyPBase) at 0.5 µg per well in six-well plates using lipofectamine™ 3000 transfection reagent (Invitrogen™). Stably transfected cells were then isolated by fluorescence-activated cell sorting (FACS).

Cell Growth Assay: Gain of function assays: 3T3 or SHSY-5Y cells expressing *GFP*, *H19*, *H19-GL*, or *DLK1* were used to measure proliferation rates. SHSY-5Y (5× 103cells / well) and 3T3 (5*10^3cells/well) cells were seeded in 96-well plates with 2.5 % serum media for 24, 48, and 72hrs. Loss of function assays: SHSY-5Y cells transfected with siRNAs (as described below) were assayed for relative growth 48 hours post-transfection. Cas9-expressing SHSY-5Y or SK-N-F1 were transfected with relevant gRNA constructs (as described below) and assayed for gain or loss of fluorescent cells three days post-transfection. The WST-8 cell proliferation assay kit (Cayman Chemical) was then used to measure cell growth differences at 450 nm absorbance. Relative growth rates were calculated in comparison to the 24-hour time point.

Short interfering RNA (siRNA)Transfection: 3T3 (5*10^5 cells/well) and SHSY-5Y (5*10^5 cells/well) cells were transfected with 25 pmol siRNA (described below) using Lipofectamine RNAiMAX transfection reagent (Invitrogen) according to the manufacturer's instructions into six-well plates. Forty-eight hours post-transfection, cells were harvested, and RNA was isolated using the TRIzol™ reagent. Subsequently, cDNA was synthesized using the Verso™ cDNA kit. All of the siRNAs were acquired from IDT.

siRNA	sense template sequence	anti-sense template sequence
Control siRNA	CGUUAAUCGCGUAUAAUACGCGUAT	AUACGCGUAUUAUACGCGAUUAACGAC
DLK1 siRNA 13.1	CUCUUAAUGCAUGAUACAGAAUAAT	AUUAUUCUGUAUCAUGCAUUAAGAGAG
DLK1 siRNA 13.2	AAAAUGGAUUCUGCGAGGAUGACAA	UUGUCAUCCUCGCAGAAUCCAUUUUGG
H19 siRNA 13.2	ACCUGACUCAGGAAUCGGCUCUGGA	UCCAGAGCCGAUUCCUGAGUCAGGUAG
H19 siRNA 13.3	CAAGCAUUCCAUUACGCCCCAUCTC	GAGAUGGGGCGUAAUGGAAUGCUUGAA

CRISPR/Cas-9 gene knockout: SHSY-5Y and SKNF1 cells were stably transfected with a Cas9 expressing Piggybac plasmid (pPB[Exp]-TagBFP2/Neo-hPGK>hCas9) using Lipofectamine™ 3000 transfection reagent (Invitrogen) and a transposase plasmid (pRP[Exp]-mCherry-CAG>hyPBase) as described above. Guide RNAs were designed as previously described[8]. SHSY-5Y:Cas9 and SKNF1:Cas9 cells (50,000 cells/well) were transfected with 1 ug of appropriate gRNA vectors in 6-well plates on day 0. Cells were analyzed for percent fluorescence on days 1 and 3, and relative fluorescence on day 3 vs. day 1 was used to determine growth differences.

Let-7 Target enrichment: SHSY-5Y cells expressing *GFP*, H19, or *H19-GL* were plated in 6-well plates. After 48 hours, cells were harvested, RNA was isolated, and RT-qPCR analysis of stated let-7 targets was performed using the SYBR green RT-qPCR system. Relative gene expression was determined using the delta-delta CT method.

RNA-Seq: Total RNA was submitted to LC Sciences (Houston, TX, USA) for library prep and sequencing. Sequencing (without spike-ins) was performed at a depth of 40 million 150 bp paired-end reads. Reads were normalized as Fragments Per Kilobase of transcript per Million mapped reads (FPKM). RNA-Seq data sets are (will be) available under the GEO reference series GSE). CHLA-15, CHLA-20, KAN, KANR, KCN, KCNR, CHLA-42, and SKNF1 were submitted for sequencing in biological duplicate.

Secondary analysis: Gene expression graphs, volcano plots, Cox regression analysis, and Kaplan–Meier curves analysis of human NB patients were generated using the data analysis tool suite on the r2: Genomics Analysis and Visualization Platform. The SEQC-498 human NB patient dataset from "An Investigation of Biomarkers Derived from Legacy Microarray Data for Their Utility in the RNA-Seq Era" was used for human NB patient analysis. HR NB patients from the Kocak 649 (GSE45547) study were identified as patients with stage 4 disease, >18 months at diagnosis, and patients of any age and stage with *M-Non* tumors. Shifts in differentially expressed chromosome-specific genes were represented as volcano plots for each chromosome. Volcano plots were generated gene lists generated using the UC Santa Cruz genome browser. Expression patterns of these gene lists were then obtained from both SEQC-498 (GSE62564) and Kocak 649 (GSE45547) studies on the r2 platform for NB subgroup comparisons.

Acknowledgments

This study was supported by a Cancer Prevention and Research Institute of Texas Grant, RR180034 (PI J.T.P).

References

1. Irwin MS, Naranjo A, Zhang FF, et al. Revised Neuroblastoma Risk Classification System: A Report From the Children's Oncology Group. *Journal of Clinical Oncology*. 2021;39(29):3229-3241. doi:10.1200/JCO.21.00278
2. DuBois SG, Macy , Margaret E., Henderson TO. High-Risk and Relapsed Neuroblastoma: Toward More Cures and Better Outcomes. *American Society of Clinical Oncology Educational Book*. 2022;(42):768-780. doi:10.1200/EDBK_349783
3. Williams LA, Spector LG. Survival Differences Between Males and Females Diagnosed With Childhood Cancer. *JNCI Cancer Spectr*. 2019;3(2). doi:10.1093/jncics/pkz032
4. Yan P, Qi F, Bian L, et al. Comparison of Incidence and Outcomes of Neuroblastoma in Children, Adolescents, and Adults in the United States: A Surveillance, Epidemiology, and End Results (SEER) Program Population Study. *Med Sci Monit*. 2020;26:e927218. doi:10.12659/MSM.927218
5. Maris JM, Guo C, White PS, et al. Allelic deletion at chromosome bands 11q14-23 is common in neuroblastoma. *Med Pediatr Oncol*. 2001;36(1):24-27. doi:10.1002/1096-911X(20010101)36:1<24::AID-MPO1007>3.0.CO;2-7
6. Attiyeh E, London W, Mosse YP, et al. Chromosome 1p and 11q deletions and outcome in neuroblastoma. *New England Journal of Medicine*. 2005;353(21):2243-2253. Accessed November 13, 2014. http://www.nejm.org/doi/full/10.1056/nejmoa052399
7. Kallen AN, Zhou XB, Xu J, et al. The Imprinted H19 LncRNA Antagonizes Let-7 MicroRNAs. *Mol Cell*. 2013;52(1):101-112. doi:10.1016/j.molcel.2013.08.027
8. Powers JT, Tsanov KM, Pearson DS, et al. Multiple mechanisms disrupt the let-7 microRNA family in neuroblastoma. *Nature*. 2016;535(7611):246-251. doi:10.1038/nature18632
9. Johnsen JI, Dyberg C, Wickström M. Neuroblastoma—A Neural Crest Derived Embryonal Malignancy. *Front Mol Neurosci*. 2019;12. doi:10.3389/fnmol.2019.00009
10. Tsubota S, Kadomatsu K. Origin and mechanism of neuroblastoma. *Oncoscience*. 2017;4(7-8):70-72. doi:10.18632/oncoscience.360
11. Liang WH, Federico SM, London WB, et al. Tailoring Therapy for Children With Neuroblastoma on the Basis of Risk Group Classification: Past, Present, and Future. *JCO Clin Cancer Inform*. 2020;(4):895-905. doi:10.1200/CCI.20.00074
12. Irwin MS, Naranjo A, Zhang FF, et al. Revised Neuroblastoma Risk Classification System: A Report From the Children's Oncology Group. *Journal of Clinical Oncology*. 2021;39(29):3229-3241. doi:10.1200/JCO.21.00278
13. Tas ML, Nagtegaal M, Kraal KCJM, et al. Neuroblastoma stage 4S: Tumor regression rate and risk factors of progressive disease. *Pediatr Blood Cancer*. 2020;67(4). doi:10.1002/pbc.28061

14. Nickerson HJ, Matthay KK, Seeger RC, et al. Favorable Biology and Outcome of Stage IV-S Neuroblastoma With Supportive Care or Minimal Therapy: A Children's Cancer Group Study. *Journal of Clinical Oncology*. 2000;18(3):477-477. doi:10.1200/JCO.2000.18.3.477
15. Colon NC, Chung DH. Neuroblastoma. *Adv Pediatr*. 2011;58(1):297-311. doi:10.1016/j.yapd.2011.03.011
16. Cohn SL, Pearson ADJ, London WB, et al. The International Neuroblastoma Risk Group (INRG) classification system: an INRG Task Force report. *J Clin Oncol*. 2009;27(2):289-297. doi:10.1200/JCO.2008.16.6785
17. Otte J, Dyberg C, Pepich A, Johnsen JI. MYCN Function in Neuroblastoma Development. *Front Oncol*. 2021;10. doi:10.3389/fonc.2020.624079
18. He Y, Su Y, Zeng J, et al. Cancer-specific survival after diagnosis in men versus women: A pan-cancer analysis. *MedComm (Beijing)*. 2022;3(3):e145. doi:10.1002/mco2.145
19. Lopes-Ramos CM, Quackenbush J, DeMeo DL. Genome-Wide Sex and Gender Differences in Cancer. *Front Oncol*. 2020;10. doi:10.3389/fonc.2020.597788
20. Zavala VA, Bracci PM, Carethers JM, et al. Cancer health disparities in racial/ethnic minorities in the United States. *Br J Cancer*. 2021;124(2):315-332. doi:10.1038/s41416-020-01038-6
21. Holowatyj AN, Wen W, Gibbs T, et al. Racial/Ethnic and Sex Differences in Somatic Cancer Gene Mutations among Patients with Early-Onset Colorectal Cancer. *Cancer Discov*. 2023;13(3):570-579. doi:10.1158/2159-8290.CD-22-0764
22. Roush S, Slack FJ. The let-7 family of microRNAs. *Trends Cell Biol*. 2008;18(10). doi:10.1016/j.tcb.2008.07.007
23. Perini G, Milazzo G, Narayan N, Ekert PG. Letting the breaks off MYCN. *Cell Death Differ*. Published online 2016:1-2. doi:10.1038/cdd.2016.112
24. Campbell K, Siegel DA, Umaretiya PJ, et al. A comprehensive analysis of neuroblastoma incidence, survival, and racial and ethnic disparities from 2001 to 2019. *Pediatr Blood Cancer*. 2024;71(1). doi:10.1002/pbc.30732
25. SEQC/MAQC-III Consortium. A comprehensive assessment of RNA-seq accuracy, reproducibility and information content by the Sequencing Quality Control Consortium. *Nat Biotechnol*. 2014;32(9):903-914. doi:10.1038/nbt.2957
26. Kocak H, Ackermann S, Hero B, et al. Hox-C9 activates the intrinsic pathway of apoptosis and is associated with spontaneous regression in neuroblastoma. *Cell Death Dis*. 2013;4(4):e586. doi:10.1038/cddis.2013.84
27. Grossman RL, Heath AP, Ferretti V, et al. Toward a Shared Vision for Cancer Genomic Data. *New England Journal of Medicine*. 2016;375(12):1109-1112. doi:10.1056/NEJMp1607591
28. Kawano A, Hazard FK, Chiu B, et al. Stage 4S Neuroblastoma. *American Journal of Surgical Pathology*. 2021;45(8):1075-1081. doi:10.1097/PAS.0000000000001647
29. Pittaway JFH, Lipsos C, Mariniello K, Guasti L. The role of delta-like non-canonical Notch ligand 1 (DLK1) in cancer. *Endocr Relat Cancer*. 2021;28(12):R271-R287. doi:10.1530/ERC-21-0208
30. Grassi ES, Pietras A. Emerging Roles of DLK1 in the Stem Cell Niche and Cancer Stemness. *Journal of Histochemistry & Cytochemistry*. 2022;70(1):17-28. doi:10.1369/00221554211048951
31. Yang J, Qi M, Fei X, Wang X, Wang K. LncRNA H19: A novel oncogene in multiple cancers. *Int J Biol Sci*. 2021;17(12):3188-3208. doi:10.7150/ijbs.62573
32. Wu B, Zhang Y, Yu Y, et al. Long Noncoding RNA H19: A Novel Therapeutic Target Emerging in Oncology Via Regulating Oncogenic Signaling Pathways. *Front Cell Dev Biol*. 2021;9. doi:10.3389/fcell.2021.796740
33. White PS, Thompson PM, Gotoh T, et al. Definition and characterization of a region of 1p36.3 consistently deleted in neuroblastoma. *Oncogene*. 2005;24(16):2684-2694. doi:10.1038/sj.onc.1208306
34. Breen CJ, O'Meara a, McDermott M, Mullarkey M, Stallings RL. Coordinate Deletion of Chromosome 3p and 11q in Neuroblastoma Detected by Comparative Genomic Hybridization. *Cancer Genet Cytogenet*. 2000;120(1):44-49. doi:10.1016/S0165-4608(99)00252-6
35. Juan Ribelles A, Gargallo P, Ferriol C, et al. Distribution of segmental chromosomal alterations in neuroblastoma. *Clinical and Translational Oncology*. 2021;23(6):1096-1104. doi:10.1007/s12094-020-02497-2
36. Janoueix-Lerosey I, Schleiermacher G, Michels E, et al. Overall Genomic Pattern Is a Predictor of Outcome in Neuroblastoma. *Journal of Clinical Oncology*. 2009;27(7):1026-1033. doi:10.1200/JCO.2008.16.0630
37. Mlakar V, Jurkovic Mlakar S, Lopez G, Maris JM, Ansari M, Gumy-Pause F. 11q deletion in neuroblastoma: a review of biological and clinical implications. *Mol Cancer*. 2017;16(1):114. doi:10.1186/s12943-017-0686-8
38. Caron H, van Sluis P, Buschman R, et al. Allelic loss of the short arm of chromosome 4 in neuroblastoma suggests a novel tumour suppressor gene locus. *Hum Genet*. 1996;97(6):834-837. doi:10.1007/BF02346199
39. Su WT, Alaminos M, Mora J, Cheung NK, La Quaglia MP, Gerald WL. Positional gene expression analysis identifies 12q overexpression and amplification in a subset of neuroblastomas. *Cancer Genet Cytogenet*. 2004;154(2):131-137. doi:10.1016/j.cancergencyto.2004.02.009
40. Martinez-Monleon A, Kryh Öberg H, Gaarder J, et al. Amplification of CDK4 and MDM2: a detailed study of a high-risk neuroblastoma subgroup. *Sci Rep*. 2022;12(1):12420. doi:10.1038/s41598-022-16455-1

41. Roy N Van, Forus A, Myklebost O, Cheng NC, Versteeg R, Speleman F. Identification of two distinct chromosome 12-derived amplification units in neuroblastoma cell line NGP. *Cancer Genet Cytogenet*. 1995;82(2):151-154. doi:10.1016/0165-4608(95)00034-M
42. Peng F, Li TT, Wang KL, et al. H19/let-7/LIN28 reciprocal negative regulatory circuit promotes breast cancer stem cell maintenance. *Cell Death Dis*. 2017;8(1):e2569-e2569. doi:10.1038/cddis.2016.438
43. Peng F, Li TT, Wang KL, et al. H19/let-7/LIN28 reciprocal negative regulatory circuit promotes breast cancer stem cell maintenance. *Cell Death Dis*. 2017;8(1):e2569-e2569. doi:10.1038/cddis.2016.438
44. Peng F, Wang JH, Fan WJ, et al. Glycolysis gatekeeper PDK1 reprograms breast cancer stem cells under hypoxia. *Oncogene*. 2018;37(8):1062-1074. doi:10.1038/onc.2017.368
45. Su H, Xu X, Yan C, et al. LncRNA H19 promotes the proliferation of pulmonary artery smooth muscle cells through AT1R via sponging let-7b in monocrotaline-induced pulmonary arterial hypertension. *Respir Res*. 2018;19(1):254. doi:10.1186/s12931-018-0956-z
46. Lopes-Ramos CM, Quackenbush J, DeMeo DL. Genome-Wide Sex and Gender Differences in Cancer. *Front Oncol*. 2020;10. doi:10.3389/fonc.2020.597788
47. He Y, Su Y, Zeng J, et al. Cancer-specific survival after diagnosis in men versus women: A pan-cancer analysis. *MedComm (Beijing)*. 2022;3(3). doi:10.1002/mco2.145
48. R2: Genomics Analysis and Visualization Platform (http://r2.amc.nl).
49. Lecerf C, Le Bourhis X, Adriaenssens E. The long non-coding RNA H19: an active player with multiple facets to sustain the hallmarks of cancer. *Cellular and Molecular Life Sciences*. 2019;76(23):4673-4687. doi:10.1007/s00018-019-03240-z
50. Yu H, Li S, Wu S xiong, Huang S, Li S, Ye L. The prognostic value of long non-coding RNA H19 in various cancers. *Medicine*. 2020;99(2):e18533. doi:10.1097/MD.0000000000018533
51. Astuti D, Latif F, Wagner K, et al. Epigenetic alteration at the DLK1-GTL2 imprinted domain in human neoplasia: analysis of neuroblastoma, phaeochromocytoma and Wilms' tumour. *Br J Cancer*. 2005;92(8):1574-1580. doi:10.1038/sj.bjc.6602478
52. Fukuzawa R, Heathcott RW, Morison IM, Reeve AE. Imprinting, expression, and localisation of DLK1 in Wilms tumours. *J Clin Pathol*. 2005;58(2):145-150. doi:10.1136/jcp.2004.021717
53. Pittaway JFH, Lipsos C, Mariniello K, Guasti L. The role of delta-like non-canonical Notch ligand 1 (DLK1) in cancer. *Endocr Relat Cancer*. 2021;28(12):R271-R287. doi:10.1530/ERC-21-0208
54. Alipoor B, Parvar SN, Sabati Z, Ghaedi H, Ghasemi H. An updated review of the H19 lncRNA in human cancer: molecular mechanism and diagnostic and therapeutic importance. *Mol Biol Rep*. 2020;47(8):6357-6374. doi:10.1007/s11033-020-05695-x
55. Sellers ZP, Schneider G, Maj M, Ratajczak MZ. Analysis of the Paternally-Imprinted DLK1–MEG3 and IGF2–H19 Tandem Gene Loci in NT2 Embryonal Carcinoma Cells Identifies DLK1 as a Potential Therapeutic Target. *Stem Cell Rev Rep*. 2018;14(6):823-836. doi:10.1007/s12015-018-9838-5
56. Takada S. Epigenetic analysis of the Dlk1-Gtl2 imprinted domain on mouse chromosome 12: implications for imprinting control from comparison with Igf2-H19. *Hum Mol Genet*. 2002;11(1):77-86. doi:10.1093/hmg/11.1.77
57. Cavalli FMG, Remke M, Rampasek L, et al. Intertumoral Heterogeneity within Medulloblastoma Subgroups. *Cancer Cell*. 2017;31(6):737-754.e6. doi:10.1016/j.ccell.2017.05.005

Novel sex-biased outcomes in neuroblastoma are associated with distinct gene expression and chromosomal loss patterns.

Vishwa Patel*, Mariya Raleigh*, Lorraine-Rana E. Benhamou, Xin Shen, Erika C. Espinosa, Niharika R. Badi, Dennis A. Sheeter, and John T. Powers

FIGURES

Figure 1

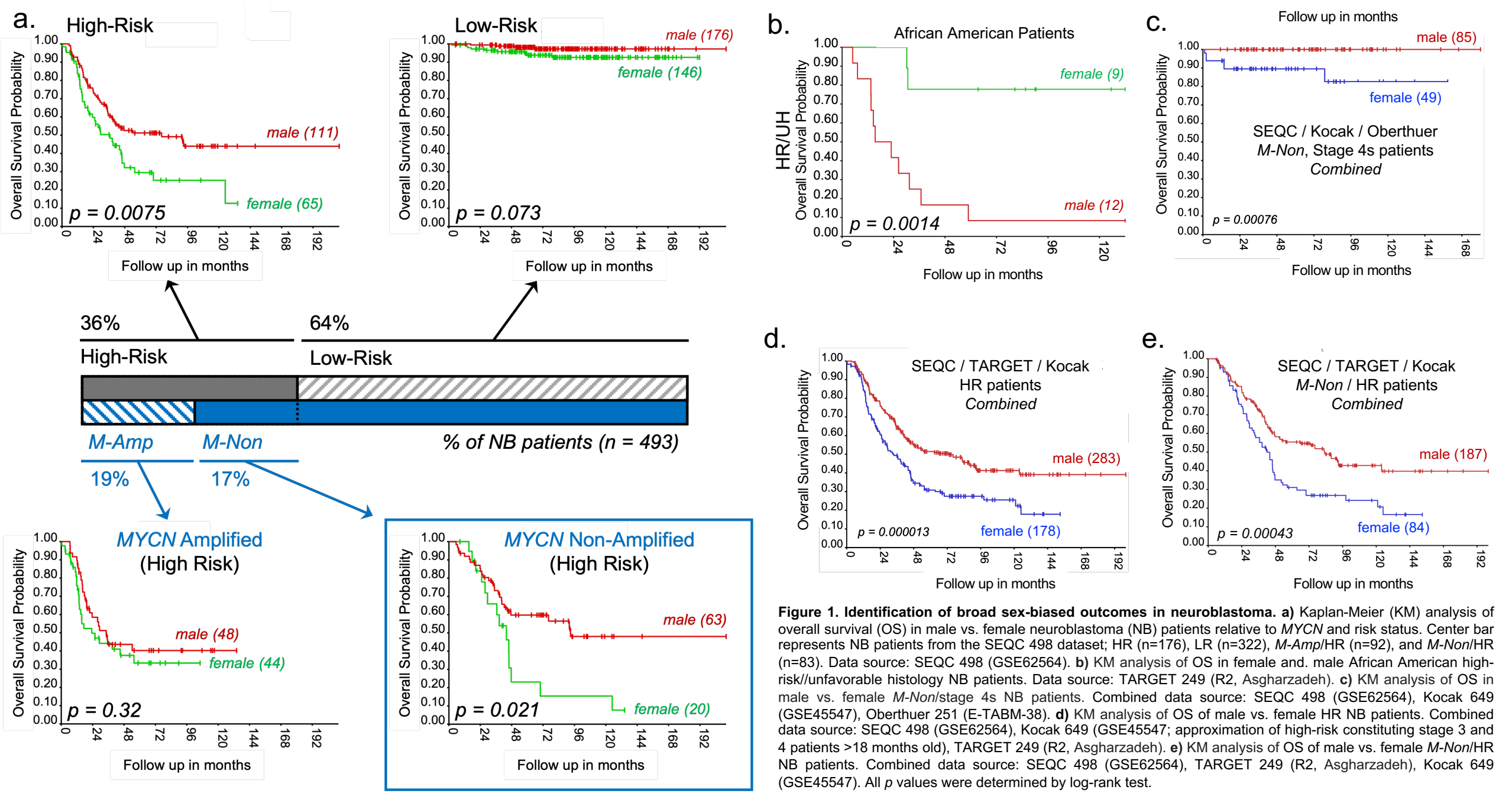

Figure 1. Identification of broad sex-biased outcomes in neuroblastoma. a) Kaplan-Meier (KM) analysis of overall survival (OS) in male vs. female neuroblastoma (NB) patients relative to *MYCN* and risk status. Center bar represents NB patients from the SEQC 498 dataset; HR (n=176), LR (n=322), *M-Amp*/HR (n=92), and *M-Non*/HR (n=83). Data source: SEQC 498 (GSE62564). **b)** KM analysis of OS in female and. male African American high-risk//unfavorable histology NB patients. Data source: TARGET 249 (R2, Asgharzadeh). **c)** KM analysis of OS in male vs. female *M-Non*/stage 4s NB patients. Combined data source: SEQC 498 (GSE62564), Kocak 649 (GSE45547), Oberthuer 251 (E-TABM-38). **d)** KM analysis of OS of male vs. female HR NB patients. Combined data source: SEQC 498 (GSE62564), Kocak 649 (GSE45547; approximation of high-risk constituting stage 3 and 4 patients >18 months old), TARGET 249 (R2, Asgharzadeh). **e)** KM analysis of OS of male vs. female *M-Non*/HR NB patients. Combined data source: SEQC 498 (GSE62564), TARGET 249 (R2, Asgharzadeh), Kocak 649 (GSE45547). All *p* values were determined by log-rank test.

Figure 2

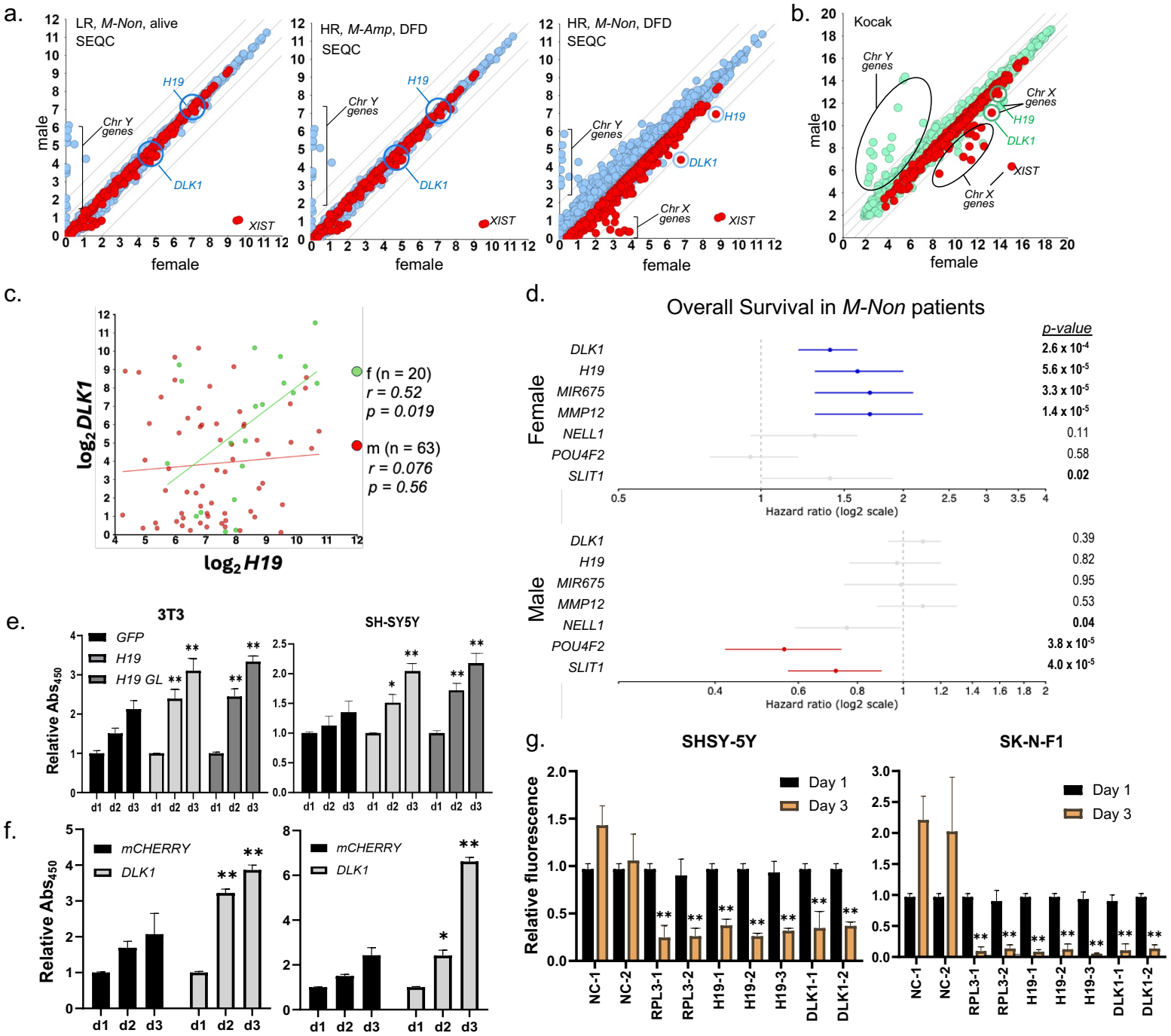

Figure 2. *H19* and *DLK1* expression differences in male vs. female neuroblastoma patients. a) X-Y plot of differential expression analysis of male vs. female NB patients. Red dots = top 500 genes most significantly upregulated in LR/*M-Non*/alive patients (left); HR/*M-Amp*/DFD patients (center); HR/*M-Non*/DFD patients (right). Data source: SEQC 498 (GSE62564). **b)** X-Y plot of differential expression analysis of male vs. female st4/*M-Non* NB patients. Red dots = top 500 significantly upregulated genes in (2a). Data source: Kocak 649 (GSE45547). **c)** X-Y plot of gene expression correlation between *H19* and *DLK1* expression levels in male and female HR/*M-Non*/DFD patients. Green line, f = females, red line, m = males. p-values determined by ANOVA. Data source: SEQC 498 (GSE62564). **d)** Cox proportional hazard regression analyses for female vs. male *M-Non* NB patients (as labeled). Selected genes are most significantly upregulated non-X Chr-associated genes in *M-Non* NB patients. Extended lines from central dots indicate 95% CI. Blue line = significant correlation > 1.0, red line = significant correlation < 1.0. Data source: SEQC 498 (GSE62564). **(e)** and **(f)** Colorimetric growth assays on 3T3 and SHSY-5Y cells relative to GFP construct-based expression of *H19, H19-GL* and *DLK1*. Significance determined by two-way ANOVA, followed by Dunnett's multiple comparison test; bars represent average +/- SEM; *p<0.05, **p<0.01, <0.001, <0.0001. **g)** CRISPR/Cas9 mediated gene knockout of *H19* and *DLK1* in SHSY-5Y and SK-N-F1 cells. Cells were transfected on d0 with control, *DLK1* and *H19* gRNAs. Loss of *H19* and *DLK1* targeted with gRNAs against negative control gRNA were measured at d1 and d3 via flow cytometry. Significance determined by two-way ANOVA, followed by Sidak's multiple comparison tests; bars represent mean+/-SEM; *p<0.05, **p<0.01, <0.001, <0.0001.

Figure 3

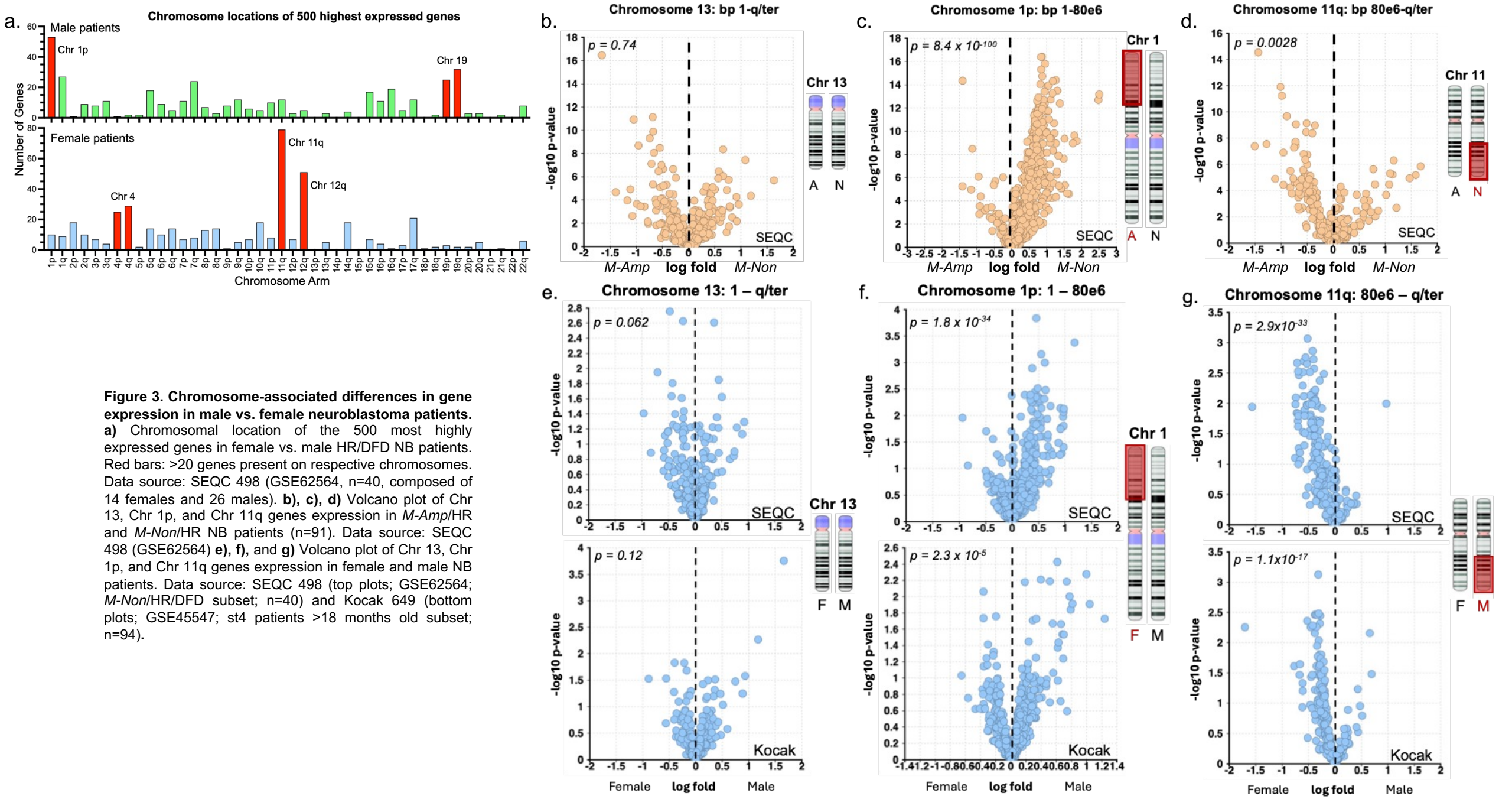

Figure 3. Chromosome-associated differences in gene expression in male vs. female neuroblastoma patients. **a)** Chromosomal location of the 500 most highly expressed genes in female vs. male HR/DFD NB patients. Red bars: >20 genes present on respective chromosomes. Data source: SEQC 498 (GSE62564, n=40, composed of 14 females and 26 males). **b), c), d)** Volcano plot of Chr 13, Chr 1p, and Chr 11q genes expression in *M-Amp*/HR and *M-Non*/HR NB patients (n=91). Data source: SEQC 498 (GSE62564) **e), f),** and **g)** Volcano plot of Chr 13, Chr 1p, and Chr 11q genes expression in female and male NB patients. Data source: SEQC 498 (top plots; GSE62564; *M-Non*/HR/DFD subset; n=40) and Kocak 649 (bottom plots; GSE45547; st4 patients >18 months old subset; n=94).

Figure 4

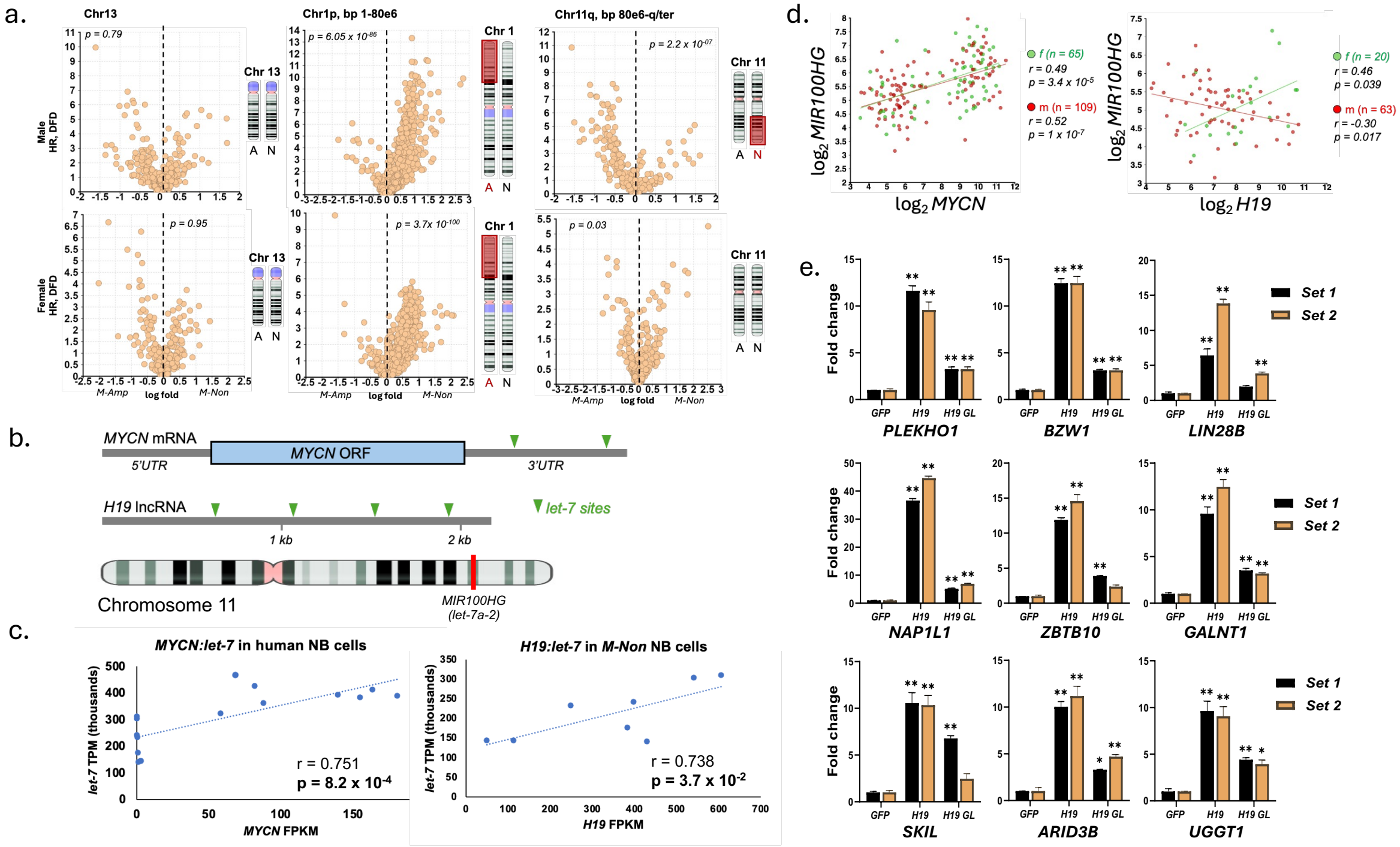
a.
Chr13
Chr1p, bp 1-80e6
Chr11q, bp 80e6-q/ter
Male HR, DFD
Female HR, DFD
p = 0.79
p = 6.05 x 10-86
p = 2.2 x 10-07
p = 0.95
p = 3.7x 10-100
p = 0.03
Chr 13
Chr 1
Chr 11
A N
M-Amp
log fold
M-Non
b.
MYCN mRNA
MYCN ORF
5'UTR
3'UTR
H19 lncRNA
let-7 sites
1 kb
2 kb
Chromosome 11
MIR100HG
(let-7a-2)
c.
MYCN:let-7 in human NB cells
let-7 TPM (thousands)
MYCN FPKM
r = 0.751
p = 8.2 x 10-4
H19:let-7 in M-Non NB cells
H19 FPKM
r = 0.738
p = 3.7 x 10-2
d.
log2 MIR100HG
log2 MYCN
f (n = 65)
r = 0.49
p = 3.4 x 10-5
m (n = 109)
r = 0.52
p = 1 x 10-7
log2 H19
f (n = 20)
r = 0.46
p = 0.039
m (n = 63)
r = -0.30
p = 0.017
e.
Fold change
GFP
H19
H19 GL
Set 1
Set 2
PLEKHO1
BZW1
LIN28B
NAP1L1
ZBTB10
GALNT1
SKIL
ARID3B
UGGT1

Figure 4

Figure 4. *H19* is strongly associated with let-7 expression in neuroblastoma. a) Volcano plots of chromosomal-linked gene expression HR dead from disease NB patients stratified by *MYCN* status and sex. Top row: plots of male *M-Non* (n=26) and *M-Amp* patients (n=26) for stated chromosomal regions; Bottom row: plots for female, *M-Non* (n=14) vs. *M-Amp* (n=25). Yellow dots: genes stemming from specified chromosomes in male or female; red box over chromosome = identified relative chromosome deficiency. Data source: Data source: SEQC 498 (GSE62564). **b)** Schematic of *MYCN* mRNA and *H19* lncRNA *let-7* sites. Green triangles = *let-7* miRNA target sites. Bottom: Location of let-7a-2 host gene (MIR100HG) on chromosome 11. **c)** Correlation plots of *MYCN* vs. *let-7* expression in human *M-Non* and *M-Amp* NB cell lines (n=16; left) and *H19* vs. *let-7* expression in human *M-Non* NB cell lines (n=8; right) were derived from NGS. Data sets will be available under the GEO reference series GSE (http://www.ncbi.nlm.nih.gov/geo/query/acc.cgi?acc=GSE (TBD1, TBD2)). p-values were derived by Pearson Product Moment Correlation (PPMC) from correlation coefficient (*r*). **d)** X-Y plots of gene expression correlation between *MYCN* and *MIR100HG* (left) in HR NB patients (left), *H19* and *MIR100HG* in *M-Non*/HR NB patients (right). Green line, f =females; red line, m =males. Data source: SEQC 498 (GSE62564; n=176); *p<0.05, **p<0.01; p-values determined by ANOVA. **e)** Expression levels of *let-7* target genes in *M-Non* SHSY-5Y cells expressing *H19* mature or full-length genetic locus (*H19-GL*). Significance determined by two-way ANOVA, followed by Sidak's multiple comparison tests; bars represent average +/- SEM; *p<0.05, **p<0.01, ***<0.001, ****<0.0001.

Supplemental Table 1

Subject	Annotation	SEQC 498	KOCAK 649	TARGET 249	OBERTHUER 251
	Total Patients	498	649	249	251
Gender	**Male**	287	344	143	146
	Female	211	268	106	105
	Unknown	-	37	-	-
Age	**< 18 months**	299	414	31	163
	> 18 months	199	235	218	85
	Unknown	-	-	-	3
***MYCN* status**	**Amplified**	92	93	68	31
	Non-Amplified	401	550	175	220
	Unknown	5	6	6	-
Risk	**Low-risk**	322	-	30	-
	High-risk	176	-	217	-
	Unknown	-	649	2	251
Stage	**1**	121	153	30	68
	2	78	113	-	46
	3	63	91	1	39
	4	183	214	216	67
	4s	53	78	-	31
	Unknown			2	-
Histology	**Favorable**	181	-	37	-
	Unfavorable	91	-	183	-
	Unknown	226	649	29	251
Death	**Yes**	105	91	140	37
	No	393	385	107	214

Neuroblastoma patient demographics and available annotations from the studies used in this manuscript.

Extended Data Figure 1

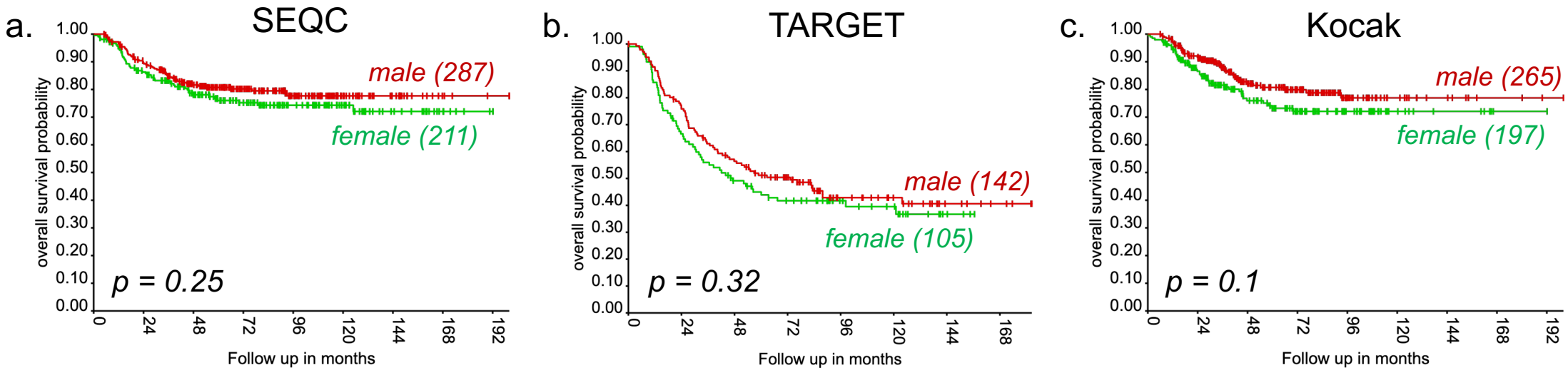

Extended Data Figure 1. Overall survival probability of male and female neuroblastoma patients across datasets. OS in male and female NB from **a)** SEQC 498 (GSE62564) cohort, **b)** TARGET 249 (R2, Asgharzadeh) cohort, and **c)** Kocak 649 (GSE45547) cohort. P-values determined by log-rank test.

Extended Data Figure 2

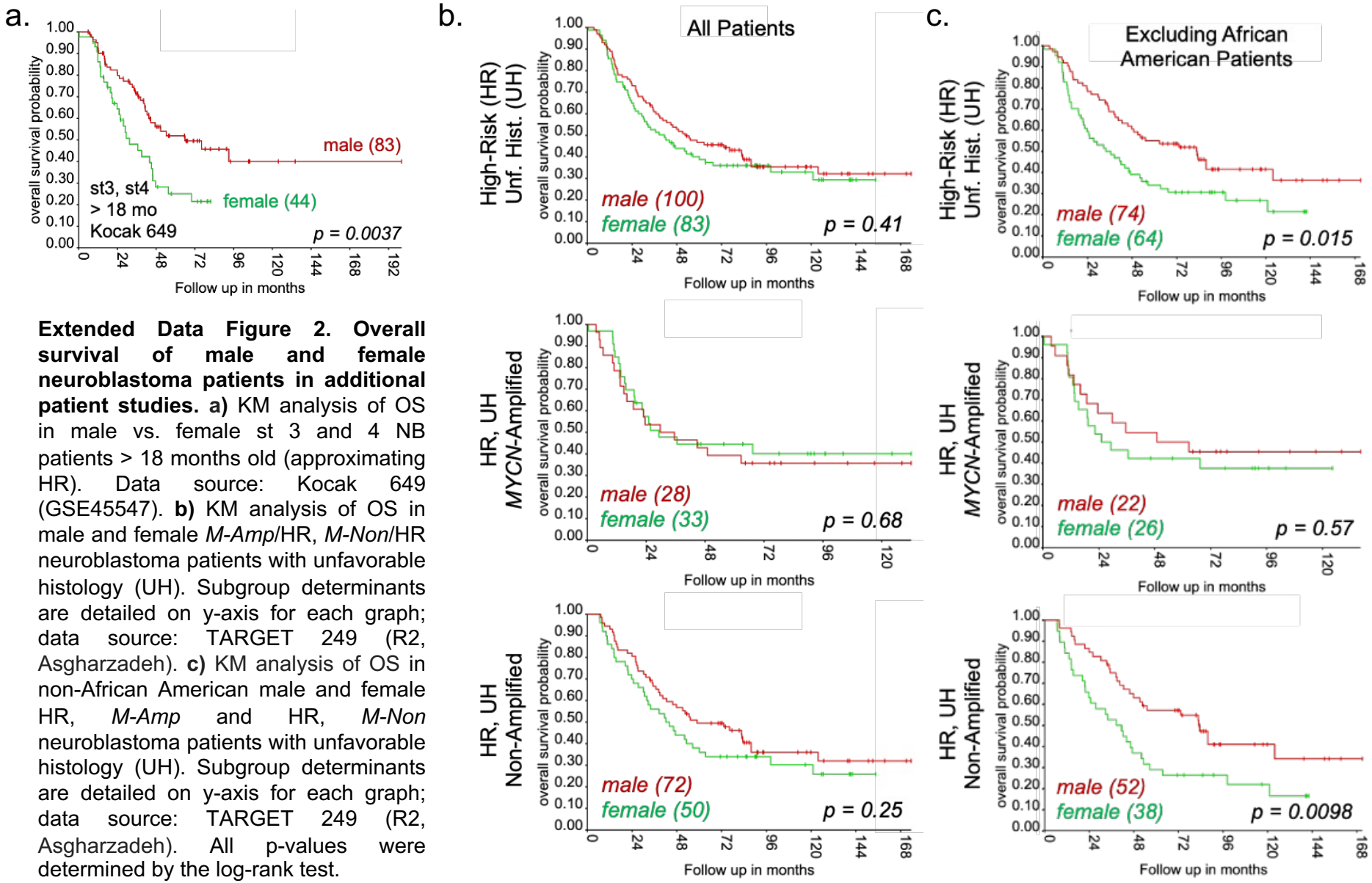

Extended Data Figure 2. Overall survival of male and female neuroblastoma patients in additional patient studies. a) KM analysis of OS in male vs. female st 3 and 4 NB patients > 18 months old (approximating HR). Data source: Kocak 649 (GSE45547). **b)** KM analysis of OS in male and female *M-Amp*/HR, *M-Non*/HR neuroblastoma patients with unfavorable histology (UH). Subgroup determinants are detailed on y-axis for each graph; data source: TARGET 249 (R2, Asgharzadeh). **c)** KM analysis of OS in non-African American male and female HR, *M-Amp* and HR, *M-Non* neuroblastoma patients with unfavorable histology (UH). Subgroup determinants are detailed on y-axis for each graph; data source: TARGET 249 (R2, Asgharzadeh). All p-values were determined by the log-rank test.

Extended Data Figure 3

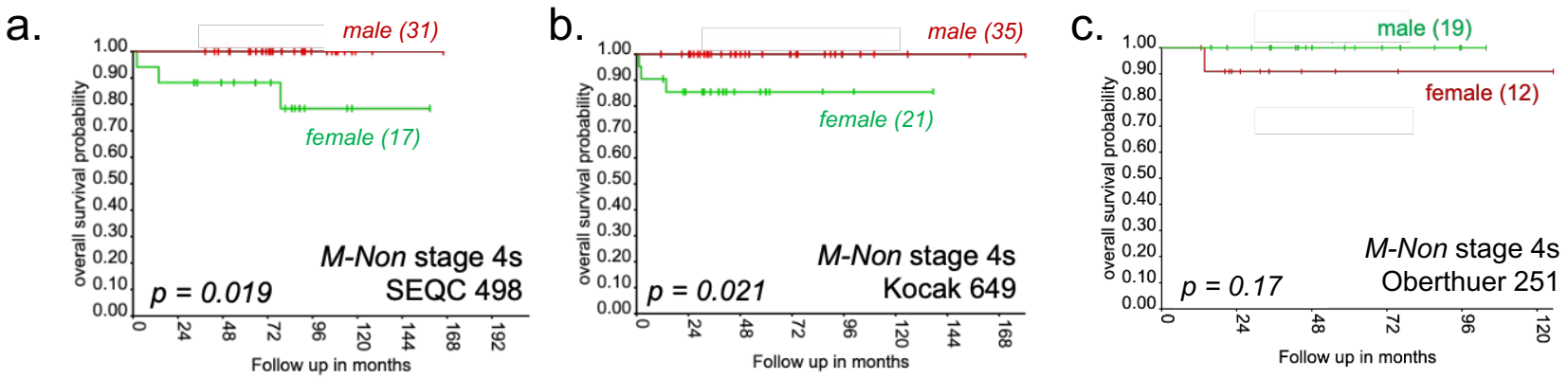

Extended Data Figure 3. Sex-biased outcomes in M-Non, stage 4s neuroblastoma. OS in male and female NB patients from **a)** SEQC 498 (GSE62564) cohort, **b)** Kocak 649 (GSE45547) cohort, and **c)**. Oberthuer 251 (E-TABM-38) cohort. p values determined by log-rank test.

Extended Data Figure 4

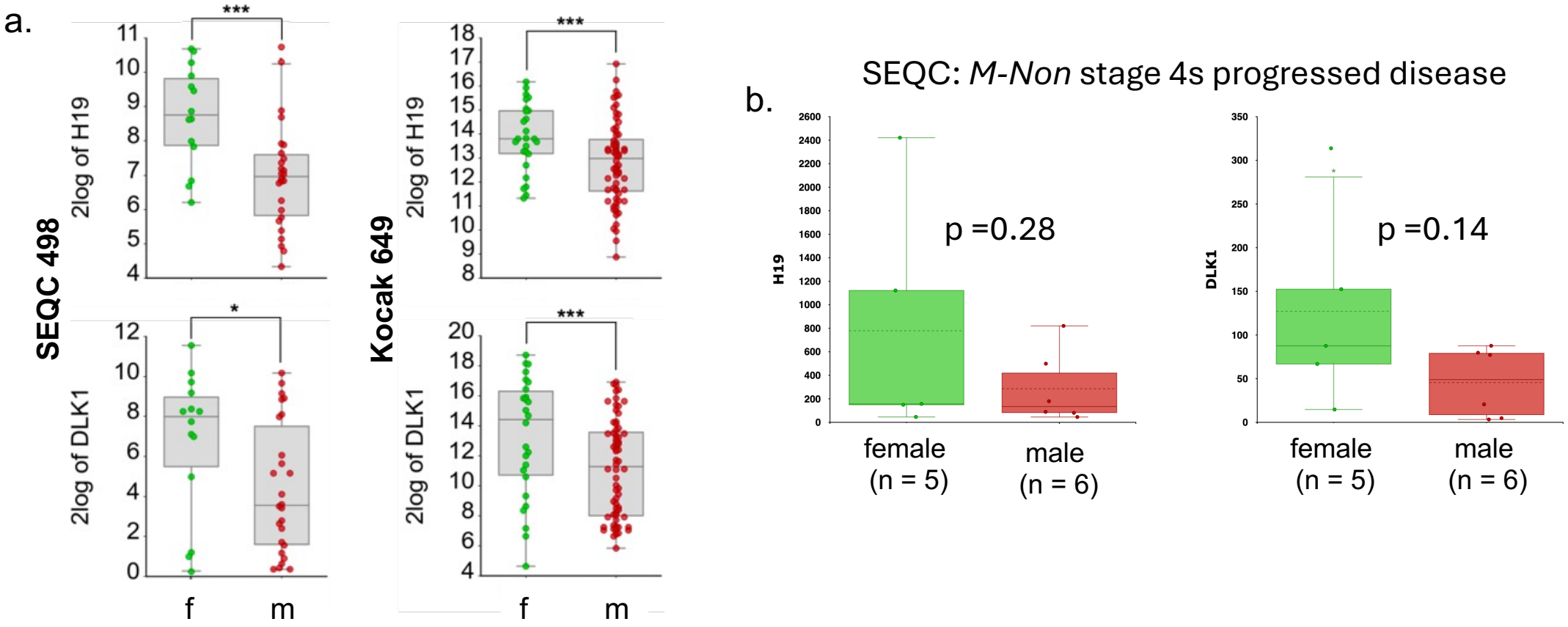

Extended Data Figure 4. *H19* and *DLK1* expression in female and male M-Non/HR patients. a) Boxplots of *H19* (top) and *DLK1* (bottom) expression in male (m; red dots) vs. female (f; green dots) patients from subsets from two datasets: SEQC 498 (left; HR/*M-Non*/DFD subset; GSE62564) and Kocak 649 (right; *M-Non*/st4 and >18 months old subset; GSE45547). *p<0.05, ***p<0.001; determined by ANOVA. **b)** Boxplots of *H19* and *DLK1* expression in male and female M-Non stage4s progressed disease patients: Data source SEQC 498. p values determined by ANOVA

Extended Data Figure 5

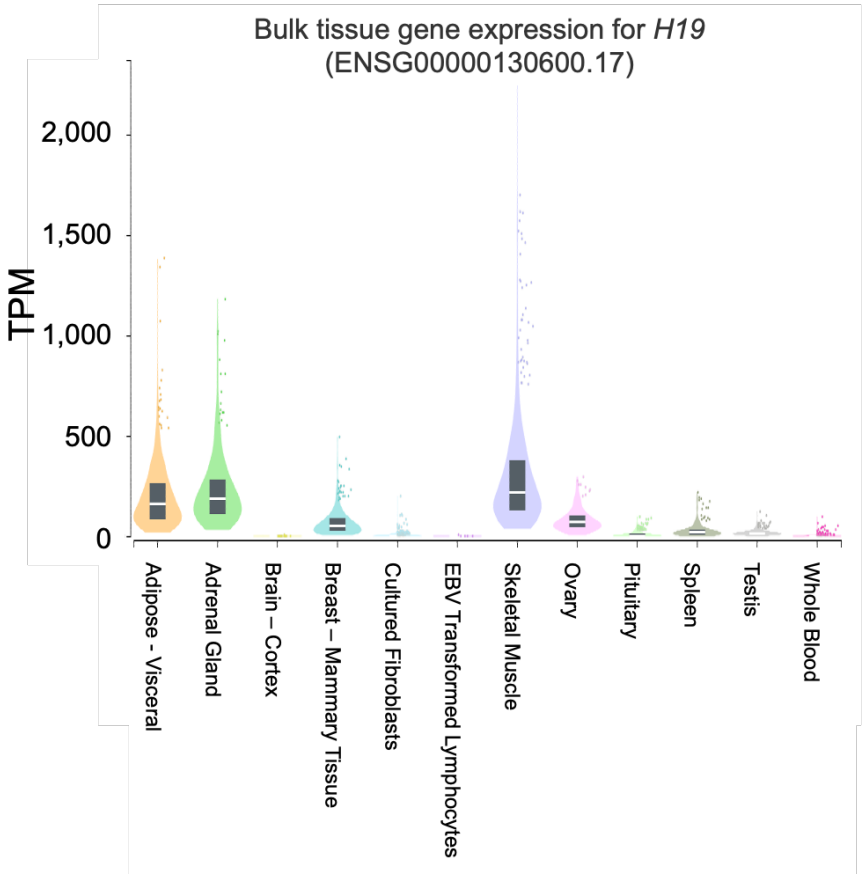

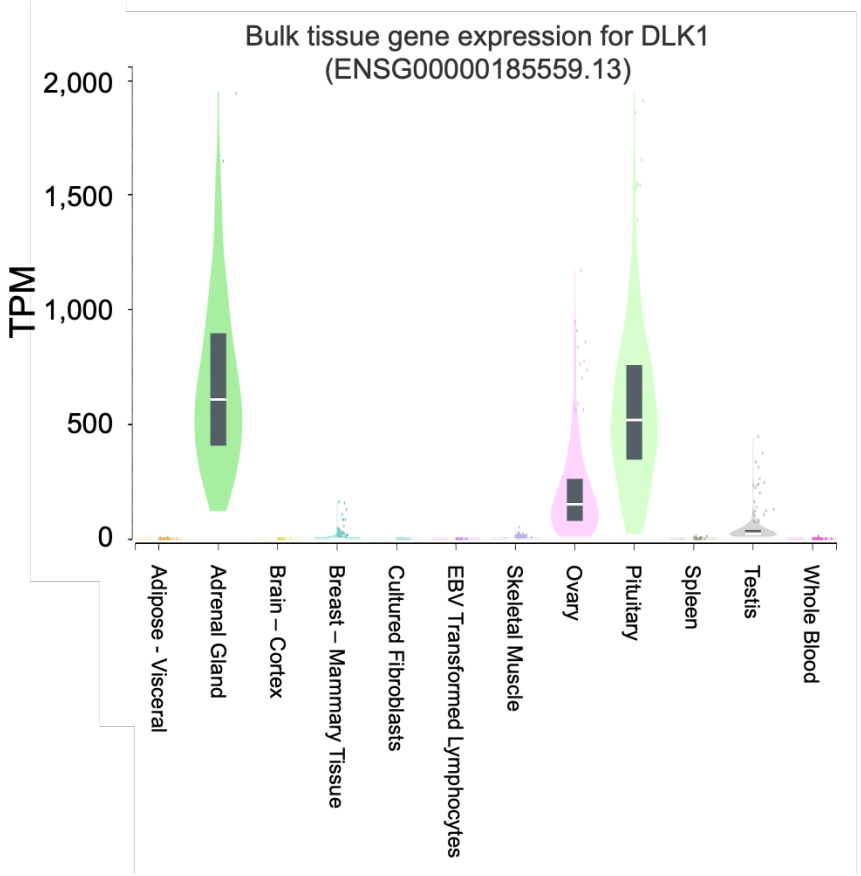

Extended Data Figure 5. *H19* and *DLK1* expression levels in normal human tissues. Expression Values are shown in Transcripts per Million (TPM). Box plots are shown as median and 25th and 75th percentiles; outliers ± 1.5x the interquartile range. Data Source: GTEx Analysis Release V8 (dbGaP Accession phs000424.v8.p2)

Extended Data Figure 6

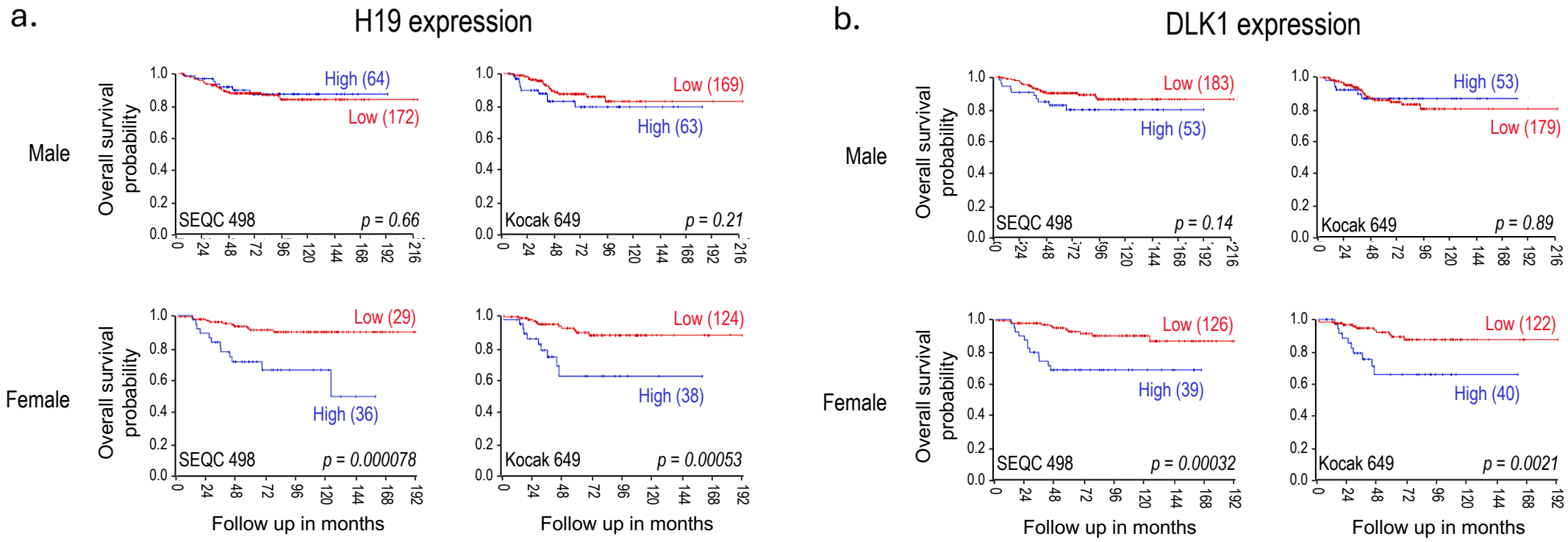

Extended Data Figure 6. Overall survival in male and female *MYCN* non-amplified neuroblastoma patients relative to *H19* or *DLK1* expression. KM plots for males (top) and females (bottom) relative to expression (high or low) levels of **a)** *H19* or **b)** *DLK1* in *M-Non* NB. Data source: SEQC 498 (GSE62564) and Kocak 649 (GSE45547); source of the graph as listed on the respective figure. Red lines = low expression; blue lines = high expression; cutoff for high/low is average expression. p-values calculated by log-rank method.

Extended Data Figure 7

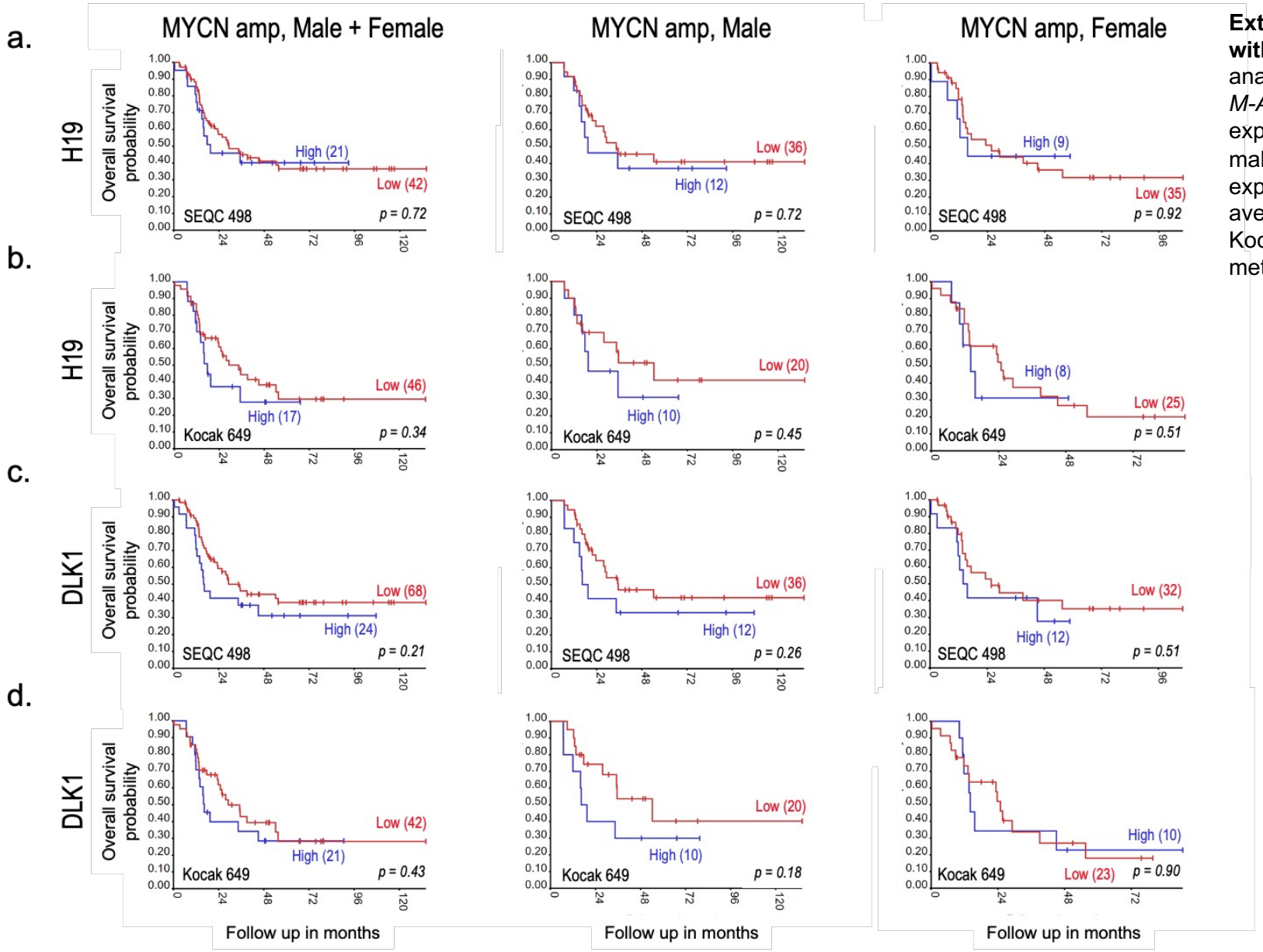

Extended Data Figure 7. *H19* and *DLK1* are not associated with overall survival in *MYCN*-amplified disease. KM analaysis of OS in two cohorts (as labeled) of male and female *M-Amp* NB patients relative to **a,b)** *H19* or **c,d)** *DLK1* expression. In each panel, plots contain males + females (left), males only (center) and females only (right). Red line = low expression; blue line = high expression; high/low cutoff is average expression. Data source: SEQC 498 (GSE62564), Kocak 649 (GSE45547), R2; p-values calculated by log-rank method.

Extended Data Figure 8

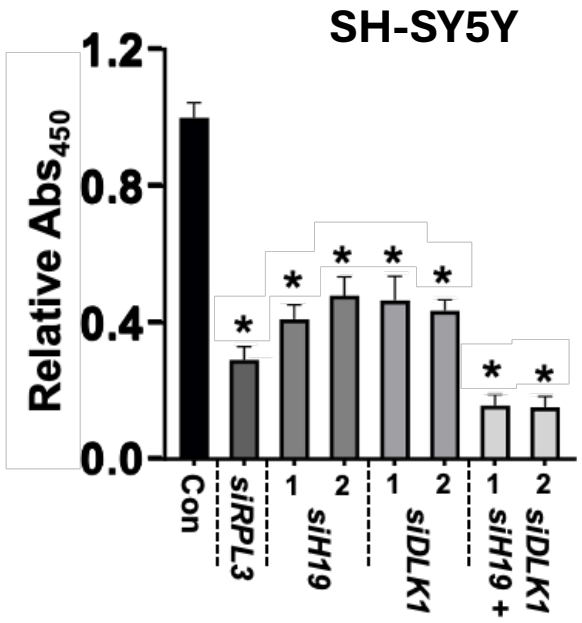

Extended Data Figure 8. Growth effects of *H19* and *DLK1* knockdown in SHSY-5Y cells. Stated siRNAs were transfected on day 0 and assayed for growth (WST-8) 48 hours later.

Extended Data Figure 9

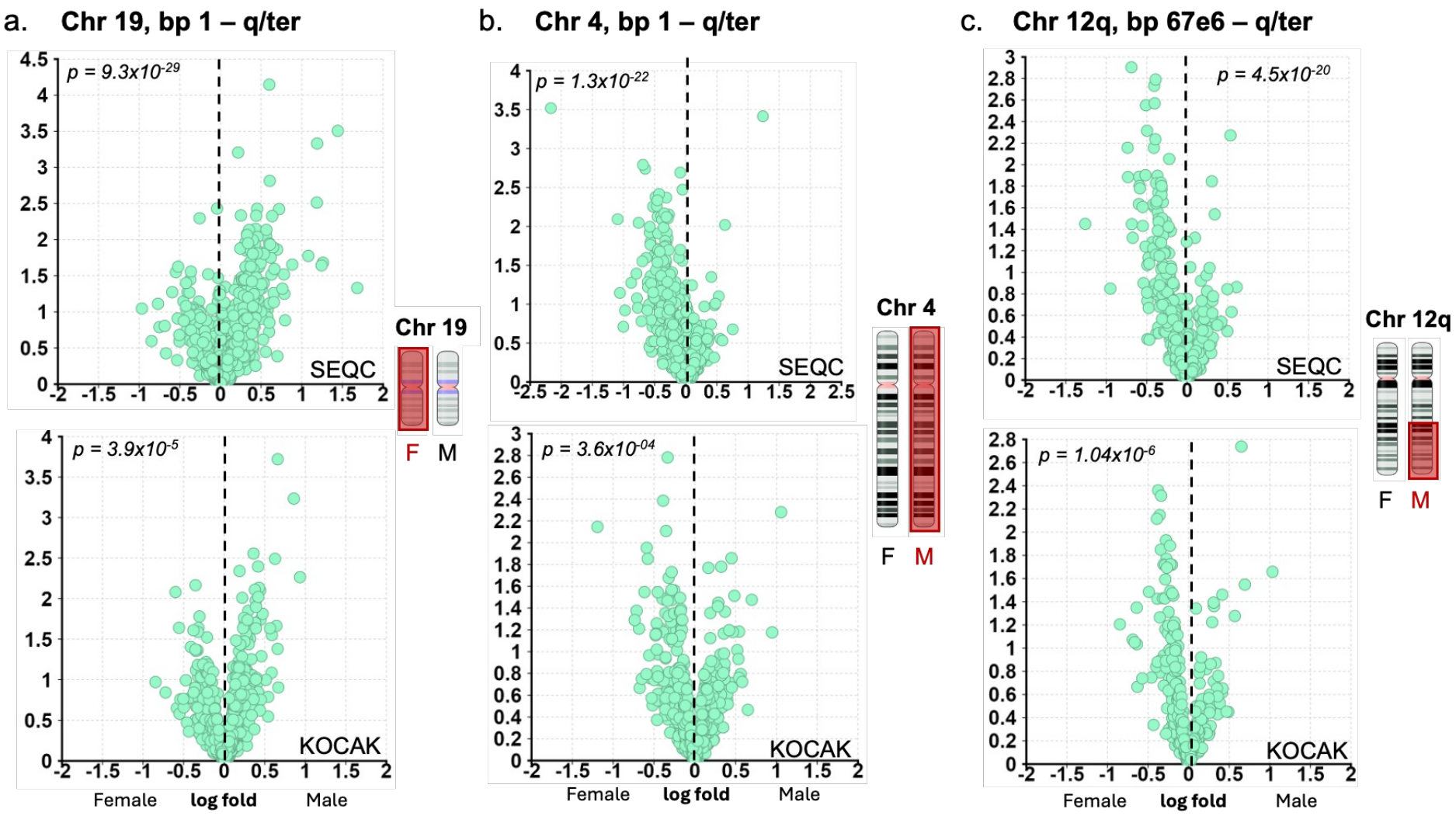

Extended Data Figure 9. Additional chromosomal-linked gene expression data from male and female high-risk NB patients dead from disease. Volcano gene expression plots of male vs. female HR, NB patients from **a)** Chr 19, bp 1 – q/ter, and **b)** Chr 4, bp 1 – q/ter and **c)** Chr 12q, bp 67e6 – q/ter**.** In all panels, green dots = genes stemming from specified chromosome; red box over chromosome = relative chromosome deficiency in neuroblastoma. Data source: SEQC 498 (GSE62564, n=40) and Kocak 649 (GSE45547, n=94), as labeled.

Extended Data Figure 10

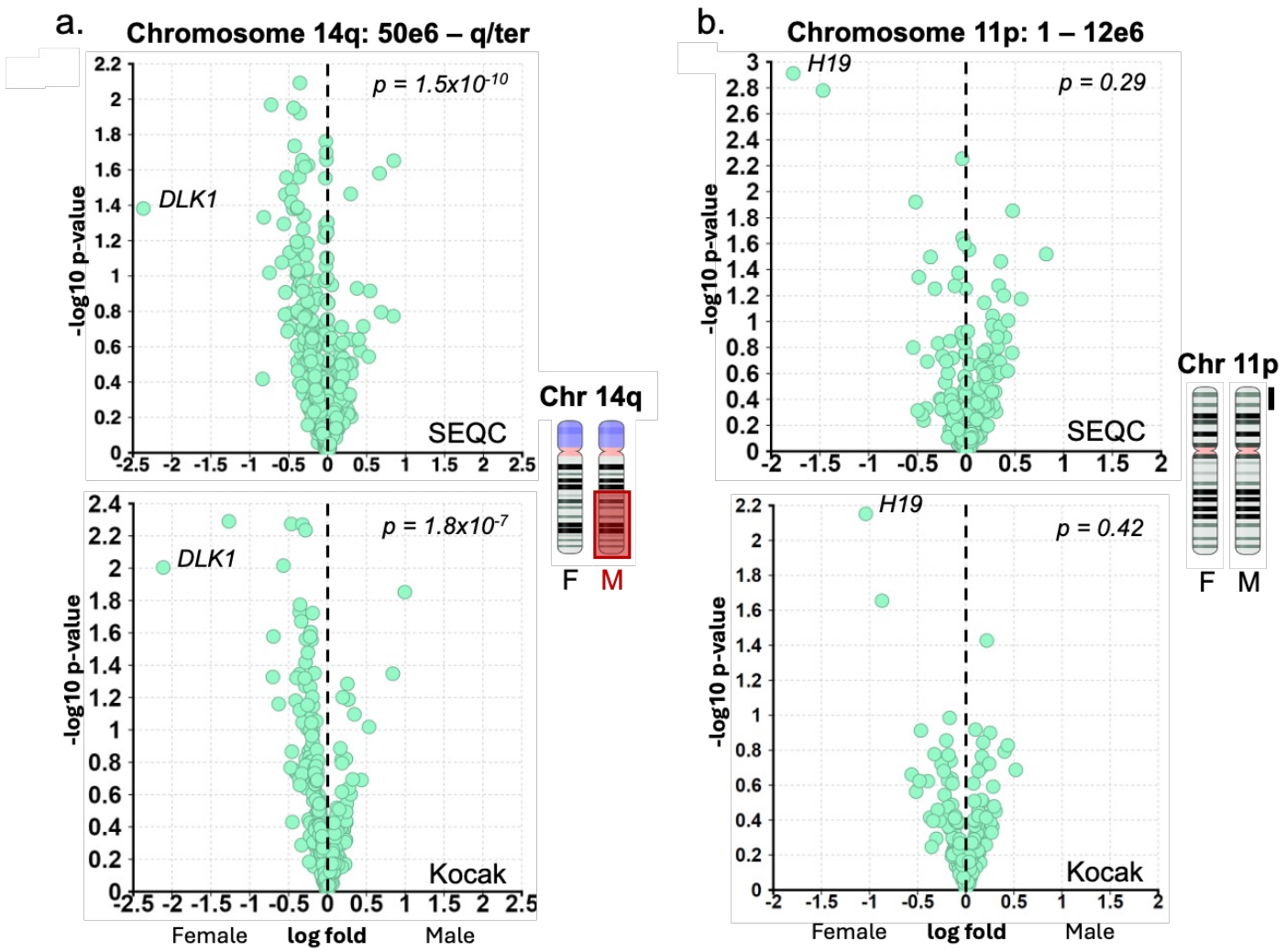

Extended Data Figure 10: Volcano plots of genes located along **a)** Chr 14 50e6 -q/ter, and **b)** chr 11q 1 – 12e6 in male vs. female HR NB patients. In all panels, green dots = genes stemming from specified chromosome; red box over chromosome = relative chromosome deficiency in neuroblastoma. Data source as labeled on the graph: SEQC 498 (top; GSE62564, *M-Non*/HR/DFD subset; n=40) and Kocak 649 (Bottom; GSE45547, st4 patients >18 months old subset; n=94).

Extended Data Figure 11

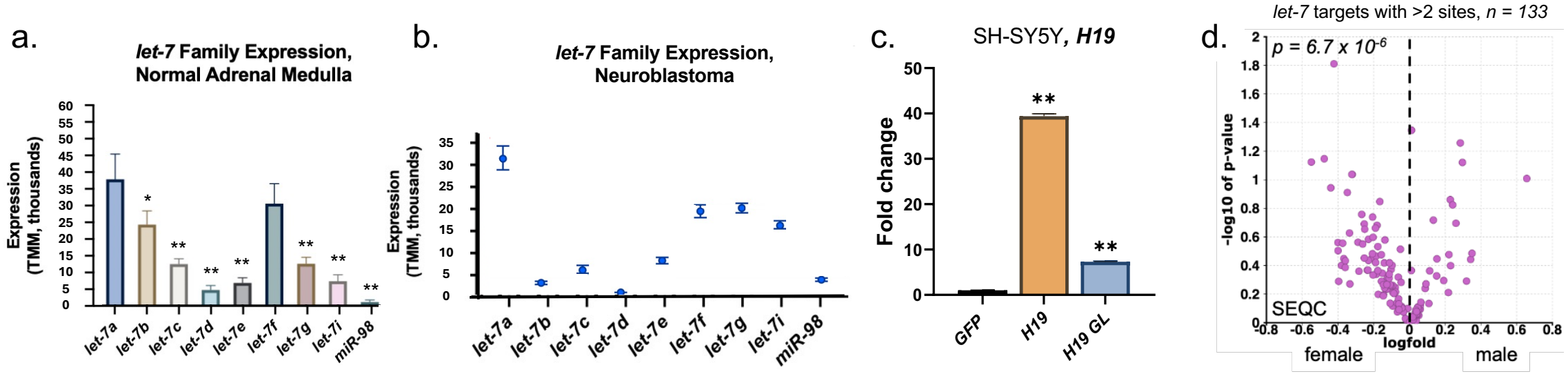

Extended Data Figure 11. a) *Let-7* family member expression in the adrenal medulla, the tissue of origin for NB. Bars represent mean+/-standard deviation. Data source is GSE29742 including the following samples (n=6): GSM737418, GSM737419, GSM737420, GSM737421, GSM737422, GSM737423. p-values determined via Dunnett's T3 Multiple Comparisons Test with *let-7a* as control; *p<0.05, **p<0.01; **b)** Mean expression of *let-7* family members in NB. Data source: Bell (GSE155945, n=97); error bars represent SEM. **c)** *H19* expression in SHSY-5Y cells transfected with *H19 and H19-GL* plasmid constructs (see *Methods*). **p<0.01 **d)** Volcano plot of differentially expressed *let-7* target mRNAs (containing >2 *let-7* sites) between female and male NB patients Data source: SEQC 498 (GSE62564; *M-Non*/HR/DFD subset; *n=40*).

Extended Data Figure 12

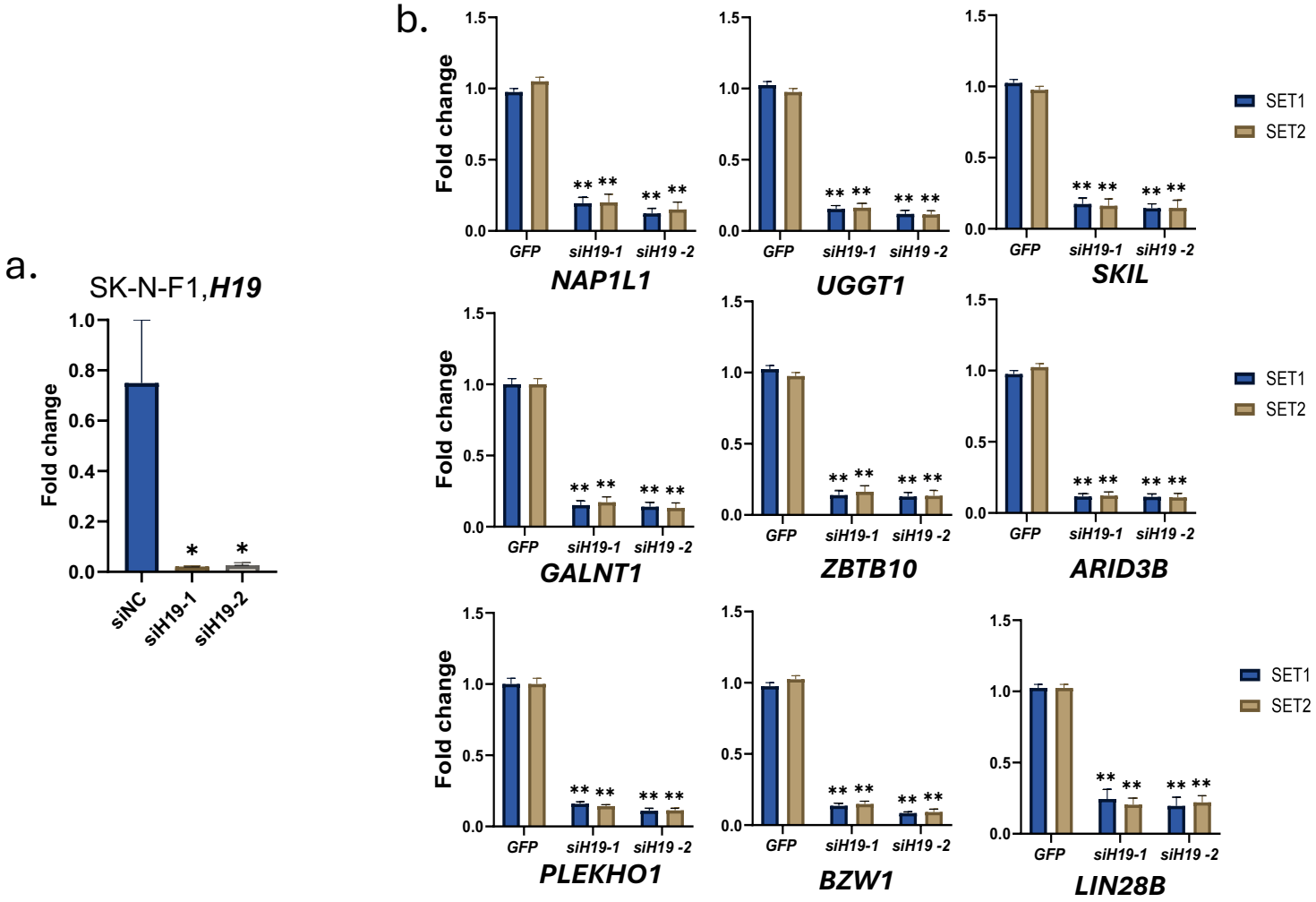

Extended Data Figure 12. a) H19 expression in *M-Non* SK-N-F1 cells in response to control siRNA or *H19* targeting siRNA transfection. **b)** Expression levels of *let-7* target genes in SK-N-F1 cells treated as in (a). Significance determined by two-way ANOVA, followed by Tukey's multiple comparison tests; bars represent average +/- SEM; **p<0.01